

## Recent advances in charm mixing and $CP$ violation at LHCb

---

**Tommaso Pajero**

*Department of Physics, University of Oxford,  
Denys Wilkinson Building, Keble Road, Oxford OX1 3RH, United Kingdom*

*E-mail:* [tommaso.pajero@physics.ox.ac.uk](mailto:tommaso.pajero@physics.ox.ac.uk)

**ABSTRACT:** After playing a pivotal role in the birth of the Standard Model in the 70's, the study of charm physics has undergone a revival during the last decade, triggered by a wealth of precision measurements from the charm and  $B$  factories, and from the CDF and especially the LHCb experiments. In this article, we sum up how the unique phenomenology of charmed hadrons can be used to test the Standard Model and we review the latest measurements performed in this field by the LHCb experiment. These include the historic first observations of  $CP$  violation and of a nonzero mass difference between the charmed neutral-meson mass eigenstates, the most precise determination of their decay-width difference to date, and a search for time-dependent  $CP$  violation reaching the unprecedented precision of  $10^{-4}$ . These results challenge our comprehension of nonperturbative strong interactions, and their interpretation calls for further studies on both the theoretical and experimental sides. The upcoming upgrades of the LHCb experiment will play a leading role in this quest.

**KEYWORDS:** Charm physics;  $CP$  violation; neutral-meson mixing; flavour-changing neutral currents.

ARXIV EPRINT: [2208.05769](https://arxiv.org/abs/2208.05769)

---

## Contents

<b>1</b>	<b>Introduction</b>	<b>1</b>
<b>2</b>	<b>Theoretical framework</b>	<b>3</b>
2.1	$D^0$ mixing	3
2.2	$CP$ violation in the decay	5
<b>3</b>	<b>The LHCb detector and charm physics</b>	<b>7</b>
3.1	Measuring $CP$ asymmetries	8
<b>4</b>	<b>Searches for <math>CP</math> violation in the decay</b>	<b>10</b>
4.1	Observation of $CP$ violation in $D^0 \rightarrow h^+h^-$ decays	10
4.2	Search for $CP$ violation in $D^0 \rightarrow K_S^0 K_S^0$ decays	14
4.3	Search for $CP$ violation in $D_{(s)}^+ \rightarrow h^0 h^+$ decays	15
4.4	Multibody decays	17
<b>5</b>	<b>Time-dependent measurements</b>	<b>19</b>
5.1	Search for time-dependent $CP$ violation in $D^0 \rightarrow h^+h^-$ decays	19
5.2	Observation of a nonzero mass difference between the neutral charmed-meson mass eigenstates with $D^0 \rightarrow K_S^0 \pi^+ \pi^-$ decays	21
5.3	Measurement of the decay-width difference of the neutral charmed-mesons mass eigenstates with $D^0 \rightarrow K^+ K^-$ and $D^0 \rightarrow \pi^+ \pi^-$ decays	24
5.4	Improvement in the knowledge of the mixing parameters	25
5.5	First simultaneous combination of charm and beauty measurements	27
<b>6</b>	<b>Conclusions and prospects</b>	<b>28</b>
	<b>References</b>	<b>30</b>

---

## 1 Introduction

Flavour physics constitutes a sensitive test bed of the standard model (SM), thanks to two peculiar properties of its Lagrangian. On the one hand, flavour changing neutral currents (FCNC) are suppressed by the Glashow–Iliopoulos–Maiani (GIM) mechanism [1, 2]. On the other, it encompasses only one observed source of violation of the  $CP$  symmetry,<sup>1</sup> that is, a single irreducible complex phase in the Cabibbo–Kobayashi–Maskawa (CKM) matrix governing the interaction of quarks with the  $W$  boson [4–6]. As a consequence,  $CP$ -violation observables are overconstrained and follow a well defined pattern. Precision

---

<sup>1</sup>A second source, ascribable to the strong interaction, is experimentally negligible [3].

measurements of FCNCs and of  $CP$  violation are thus sensitive probes for new interactions beyond the SM (BSM), which could modify their size through diagrams including particles off the mass shell, even if their energy scales are larger than those available to the current particle colliders. Historically, this line of research has turned out to be very fruitful. Notable examples include the proposal of the GIM mechanism and the prediction of the existence of the charm quark in 1970 [1], based on the suppression of the branching fraction of  $K_L^0 \rightarrow \mu^+ \mu^-$  decays [7, 8]; the observation of  $CP$  violation in  $K^0$  mesons, which suggested the existence of a third generation of quarks in 1973 [5, 9]; and the first evidence of  $B^0$  mixing, which set a lower bound on the mass of the top quark in the 80s [10, 11]. Thus, it is not unlikely that future studies of rare flavour-changing processes will shed light on the structure of the BSM interactions that are needed to explain the shortcomings of the SM, such as the missing explanation of the nature of dark matter [6] and of the cosmological baryon asymmetry [12].

Charmed hadrons are the only hadrons where precision measurements of FCNCs and of  $CP$  violation involving the decay of up-type quarks can be performed. Therefore, they are sensitive to a different class of interactions with respect to  $B$  and  $K$  mesons, where the decaying quark is of type down. Their phenomenology is also peculiar due to a stronger GIM suppression — a consequence of the smaller mass of the beauty than the top quark involved in the respective loop diagrams, and of the smallness of the CKM matrix elements connecting the first two generations of quarks with the third. In particular,  $CP$  violation is proportional to the following combination of CKM matrix elements,  $\mathcal{I}m(V_{cb}V_{ub}^*/V_{cs}V_{us}^*) \approx -6 \times 10^{-4}$  [13], leading to  $CP$  asymmetries typically of the order of  $10^{-4}$  to  $10^{-3}$  [14]. The smallness of FCNCs and of  $CP$  violation in charm has frustrated their search for a long time. It was only during the last decade that experimental progress with the  $B$  factories, the CDF experiment and, most prominently, the LHCb experiment has eventually allowed these phenomena to be observed for the first time.

The entrance of charm physics into the era of precision measurements poses several challenges not only on the experimental, but also on the theoretical side. In fact, while the enhanced GIM suppression potentially provides excellent sensitivity to BSM interactions, the theoretical interpretation of the measurements is complicated by the contributions from nonperturbative strong interactions involving strange and down quarks [15]. Not only the size of these contributions is difficult to calculate, but they are subject to large cancellations, as they vanish in the  $SU(3)_F$  limit, where the masses of the  $s$ ,  $d$  and  $u$  quarks are neglected with respect to the typical hadronic scale of charm decays,  $\Lambda_{\text{QCD}}$ . Therefore, a rigorous assessment of the agreement of the measurements with the SM will require a combination of advances of the available theoretical tools and an extensive experimental program of auxiliary measurements.

This review is structured as follows. Section 2 introduces the theoretical framework to describe mixing and  $CP$  violation in charmed hadrons and outlines the status of the theoretical predictions. An introduction to the LHCb experiment and to the typical analysis methods adopted in charm measurements is provided in section 3, before describing the most important time-integrated and time-dependent measurements performed during the last few years in sections 4 and 5, respectively. Finally, we conclude by sketching the

prospects for experimental progress in the coming years in section 6. Throughout this article, the first quoted uncertainties are statistical and the second are systematic.

## 2 Theoretical framework

The next sections provide a brief theoretical introduction to the phenomena of mixing and  $CP$  violation in the decay of charmed hadrons.

### 2.1 $D^0$ mixing

One of the most interesting phenomena involving FCNCs is mixing,<sup>2</sup> that is, the quantum oscillation of a neutral flavoured meson such as the  $D^0$  meson, made up of a  $c\bar{u}$  quark pair, into its antiparticle, and vice versa; see fig. 1. This process is parametrised through the dimensionless mixing parameters  $x_{12}$  and  $y_{12}$ , defined as  $x_{12} \equiv 2|M_{12}/\Gamma$  and  $y_{12} \equiv |\Gamma_{12}/\Gamma|$ , where  $\mathbf{H} \equiv \mathbf{M} - \frac{i}{2}\mathbf{\Gamma}$  is the effective Hamiltonian of the subspace spanned by  $|D^0\rangle$  and  $|\bar{D}^0\rangle$  and  $\Gamma$  is the  $D^0$  decay width [19–21].<sup>3</sup> The mixing parameter  $x_{12}$  ( $y_{12}$ ) is proportional to the size of the transition amplitudes between  $D^0$  and  $\bar{D}^0$  mesons through off-shell (on-shell) intermediate states, and is equal to the magnitude of the normalised difference between the masses (decay widths) of the two mass eigenstates, conventionally denoted as  $x \equiv \Delta m/\Gamma$  ( $y \equiv \Delta\Gamma/2\Gamma$ ), up to second order in the small  $CP$ -violation parameter  $\phi_{12} \equiv \arg(M_{12}/\Gamma_{12})$ . Experimentally,  $x_{12}$  and  $y_{12}$  are equal to  $(4.07 \pm 0.48) \times 10^{-3}$  and  $(6.45 \pm 0.24) \times 10^{-3}$ , respectively [22].

The absorptive mixing amplitude can be written in the SM as [21]

$$\Gamma_{12}^{\text{SM}} = \frac{(\lambda_s - \lambda_d)^2}{4}\Gamma_2 + \frac{(\lambda_s - \lambda_d)\lambda_b}{2}\Gamma_1 + \frac{(\lambda_b)^2}{4}\Gamma_0, \quad (2.1)$$

where  $\lambda_i \equiv V_{ci}V_{ui}^*$ , unitarity of the CKM matrix is assumed ( $\lambda_d + \lambda_s + \lambda_b = 0$ ), and  $\Gamma_{2,1,0}$  are the  $\Delta U_3 = 0$  matrix elements of the  $\Delta U = 2, 1, 0$  transitions, respectively.<sup>4</sup> In terms

<sup>2</sup>We refer the reader to ref. [16] for a recent review of leptonic and semileptonic decays of charmed hadrons, which are not discussed in this article, and to refs. [17, 18] for updated experimental results.

<sup>3</sup>We employ natural units throughout this article.

<sup>4</sup> $U$  spin is the  $SU(2)$  subgroup of  $SU(3)_{\text{F}}$  relating the  $d$  and  $s$  quarks.

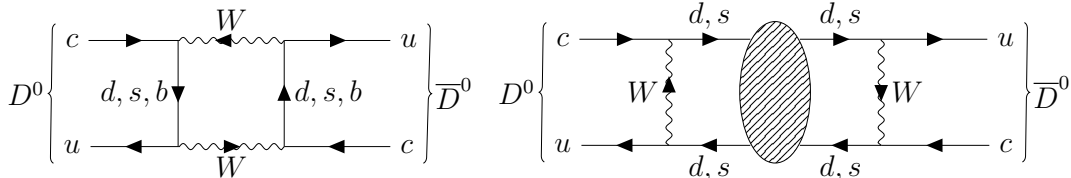


**Figure 1.** Examples of diagrams of (left) perturbative and (right) nonperturbative contributions to  $D^0$  mixing. In the right diagram, the dashed area represents low-energy QCD interactions, possibly involving the exchange of hadrons on the mass shell. The nonperturbative contributions dominate, since they avoid the suppression from the loop factor, and can have a much milder  $SU(3)_{\text{F}}$ -breaking (GIM) suppression [14].

of their flavour structure, they are equal to

$$\begin{aligned}
\Gamma_2 &= \Gamma_{dd} - 2\Gamma_{ds} + \Gamma_{ss} \sim (d\bar{d} - s\bar{s})^2 = \mathcal{O}(\epsilon^2), \\
\Gamma_1 &= \Gamma_{dd} - \Gamma_{ss} \sim (d\bar{d} - s\bar{s})(d\bar{d} + s\bar{s}) = \mathcal{O}(\epsilon), \\
\Gamma_0 &= \Gamma_{dd} + 2\Gamma_{ds} + \Gamma_{ss} \sim (d\bar{d} + s\bar{s})^2 = \mathcal{O}(1),
\end{aligned}
\tag{2.2}$$

where  $\Gamma_{ij}$  designates the absorptive part, proceeding through on-shell intermediate states, of the box diagrams with internal quarks  $i$  and  $j$ , and the rightmost terms show the order of  $\Gamma_{0,1,2}$  in terms of the  $U$ -spin breaking parameter  $\epsilon \approx 0.3$ , assuming that a perturbative expansion in this parameter is possible [23]. Owing to the hierarchy of CKM elements,  $(\lambda_s - \lambda_d)/2 \approx 0.22 - i 6.6 \times 10^{-5}$  and  $\lambda_b/2 \approx 3.0 \times 10^{-5} + i 6.6 \times 10^{-5}$ , the first term in eq. (2.1) is the dominant one, even if it arises only at second order in  $U$ -spin breaking [24, 25]. On the other hand,  $CP$  violation requires the contribution of a second amplitude with a different weak phase [6],<sup>5</sup> namely, the second term in the right-hand side of eq. (2.1) or an additional term from BSM interactions. Conventionally, it is parametrised through the phase of  $\Gamma_{12}$  with respect to its dominant  $\Delta U = 2$  component,  $\phi_2^\Gamma \equiv \arg(\Gamma_{12}/[(\lambda_s - \lambda_d)^2 \Gamma_2])$ , where the subscript denotes the chosen convention [21].

An analogous discussion and weak phase,  $\phi_2^M$ , can be defined also for the dispersive matrix element,  $M_{12}$ , describing off-shell intermediate states. The only difference is that  $M_1$  and  $M_0$  receive additional contributions,  $2(M_{sb} - M_{db})$  and  $4(M_{bb} - M_{sb} - M_{db})$ , which could compensate in part for the CKM suppression.

Providing predictions for the mixing parameters is notoriously a formidable task. Heavy quark expansion has been successfully used to predict the lifetimes of  $D^0$ ,  $D^+$  and  $D_s^+$  mesons, suggesting that an inclusive calculation from a perturbative expansion in terms of  $\Lambda_{\text{QCD}}/m_c \sim 0.3$  and of  $\alpha_s(m_c) \sim 0.33$  might be viable [26]. The individual contributions to  $y_{12}$  from single  $\Gamma_{ij}$  amplitudes are five times larger than the experimental value prior to GIM cancellations, but the size of such cancellations is not controlled yet; see ref. [27] for a review. In the very long term, the size of the mixing parameters may be predicted through lattice calculations, by building on the methods described in ref. [28]. On the contrary, exclusive approaches to estimate  $y_{12}$ , which sum over the contributions from all the final states shared by  $D^0$  and  $\bar{D}^0$  mesons [29, 30], are unlikely to provide precise predictions. In fact, the contributions from different final states within the same  $U$ -spin multiplet tend to cancel; hence, the precision with which the branching fractions and the strong phases of the decay amplitudes are known — in particular for multibody decays — significantly limits the achievable precision [24]. Moreover, since the exclusive methods are based on charm experimental data, they are unable to distinguish SM contributions from new interactions. It is, however, interesting to note that the authors of ref. [24] showed well before a nonzero value of  $y_{12}$  was measured that even only  $U$ -spin breaking from the different phase space of multibody final states, neglecting all dynamical effects, can account for a value of  $y_{12}$  as large as 1%, which is consistent with the experimental value [31]. Finally, a dispersion

---

<sup>5</sup>Weak phases are defined as the phases that change their sign under the  $CP$  transformation, like those of the CKM matrix elements. On the other hand, phases that do not change their sign under the  $CP$  transformation, such as those arising from QCD, are called strong phases.

relation between the mixing parameters has been derived in ref. [32] in the heavy-quark limit, predicting values of  $x_{12}$  between  $10^{-3}$  and  $10^{-2}$  if  $y_{12}$  is of the order of 1%, in keeping with the experimental data.

As far as  $CP$  violation is concerned, the phases  $\phi_2^M$  and  $\phi_2^\Gamma$  can be estimated from eq. (2.1) to be of the order of 2 mrad, though enhancements of up to one order of magnitude cannot be excluded [21, 33–35]. An upper bound of 5 mrad has recently been argued for  $\phi_2^\Gamma$  [21]. The experimental limits are less precise by one order of magnitude, as the weak phases are currently measured to be  $\phi_2^M = (0.030 \pm 0.021)$  rad and  $\phi_2^\Gamma = (0.044 \pm 0.027)$  rad [22].

Even in absence of precise SM predictions, the small size of mixing and  $CP$  violation parameters can be employed to set stringent limits on the scale of new BSM interactions, up to more than  $10^4$  TeV, by assuming that contributions BSM saturate the measured values of  $x_{12}$  and  $\phi_2^M$  [36–41].

## 2.2 $CP$ violation in the decay

$CP$  violation can arise also in the decay amplitudes, where it is conventionally quantified through the parameter

$$a_f^d \equiv \frac{|A_f|^2 - |\bar{A}_{\bar{f}}|^2}{|A_f|^2 + |\bar{A}_{\bar{f}}|^2}, \quad (2.3)$$

where  $A_f$  and  $\bar{A}_{\bar{f}}$  denote the decay amplitudes of a charmed hadron and of the corresponding anti-hadron into the  $CP$ -conjugate final states  $f$  and  $\bar{f}$ , respectively. This phenomenon is expected to be observable only in singly Cabibbo-suppressed (SCS)  $c \rightarrow us\bar{s}$  and  $c \rightarrow ud\bar{d}$  transitions, which receive contributions from QCD penguin and chromomagnetic-dipole operators. In contrast, Cabibbo-favoured (CF)  $c \rightarrow us\bar{d}$  and doubly Cabibbo-suppressed (DCS)  $c \rightarrow ud\bar{s}$  transitions cannot be influenced by these operators, as they involve quarks of four different flavours. Therefore, any signs of  $CP$  asymmetries larger than  $10^{-5}$  in CF or DCS decays would be an unambiguous evidence of new BSM interactions [14, 42]. The only exception is that of CF decays that contain an odd number of  $K_S^0$  kaons in their final state, since these decays also receive a contribution from a DCS amplitude, whose interference with the CF amplitude may enhance the  $CP$  asymmetry up to  $10^{-4}$  level [43].

To predict the size of  $a_f^d$ , it is useful to decompose the decay amplitude in terms of CKM factors as

$$A_f \equiv A_{sd} \frac{\lambda_s - \lambda_d}{2} - A_b \frac{\lambda_b}{2}, \quad (2.4)$$

where only two terms appear thanks to CKM unitarity, and the choice of using  $(\lambda_s - \lambda_d)/2$  for the first is dictated by  $U$ -spin symmetry arguments. While  $A_{sd}$  is in some cases dominated by tree diagrams, it can receive contributions also from exchange, annihilation and broken-penguin (annihilation) diagrams, where the broken penguin is the  $U$ -spin breaking difference of the penguin diagrams with internal quarks  $s$  and  $d$ . Analogously, also  $A_b$  contains all the categories listed above, with the exception that broken penguins are substituted by penguin diagrams with internal quark  $b$  and by the  $U$ -spin conserving average of penguin diagrams with internal quarks  $s$  and  $d$  [44, 45].

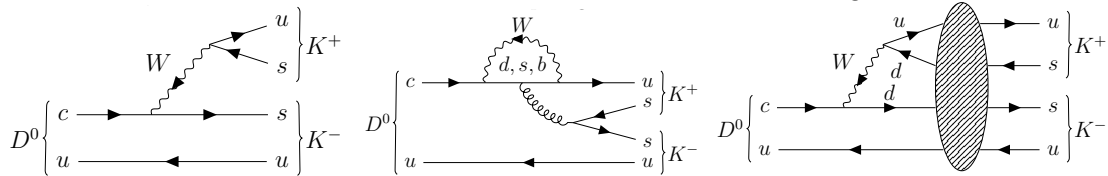


**Figure 2.** Examples of diagrams contributing to the  $D^0 \rightarrow K^+ K^-$  decay. The tree diagram (left) is proportional to  $\lambda_s$ , while the penguin diagram (centre) is proportional to  $\lambda_q$ , where  $q$  is the internal quark of the loop. The right diagram represents rescattering of an on-shell state including a  $d\bar{d}$  quark pair such as  $\pi^+ \pi^-$ , represented by the dashed area, into the  $K^+ K^-$  final state. This diagram is proportional to  $\lambda_d$  and thus contributes to  $A_{sd}$  ( $A_b$ ) with a relative minus sign (with the same sign) as the tree diagram. Therefore, it gives rise to  $CP$  violation if it has a different strong phase with respect to the tree diagram, as expected from rescattering.

The action of the  $CP$  transformation corresponds to the complex conjugation for the CKM matrix elements, while it has no effects on the strong matrix elements  $A_{sd}$  and  $A_b$ . Therefore, the  $CP$  violation in the decay is equal to

$$a_f^d \approx \mathcal{I}m \left( \frac{2\lambda_b}{\lambda_s - \lambda_d} \right) \mathcal{I}m \left( \frac{A_b}{A_{sd}} \right) = (-5.8 \pm 0.2) \times 10^{-4} \left| \frac{A_b}{A_{sd}} \right| \sin \delta, \quad (2.5)$$

where terms of order higher than one in  $\lambda_b$  are neglected, the CKM factor is taken from ref. [13], and the strong-phase difference  $\delta$  is defined as  $\delta \equiv \arg(A_b/A_{sd})$ . Since the second term in eq. (2.4) is heavily CKM suppressed, the decay width into a given final state is described to excellent approximation by the first term only, and the magnitude of  $A_{sd}$  can be calculated from the branching fraction of the decay. Thus, to provide predictions for  $a_f^d$ , one then needs to estimate the size of  $A_b$  and of  $\delta$ . Penguin diagrams are naively suppressed by a factor of  $\alpha_s/\pi$  with respect to the tree diagrams [14], leading to an additional suppression of  $a_f^d$  by approximately a factor of 5 on top of the already small CKM factor. However, final-state rescattering from nonperturbative strong interactions is topologically equivalent to a penguin diagram, see fig. 2, and could enhance this prediction by up to one order of magnitude, leading to asymmetries of the order of  $10^{-3}$  [15, 46]. Even larger enhancements may take place in decays into two neutral kaons, where  $CP$  violation is expected to arise from the interference of the tree-level transitions  $c\bar{u} \rightarrow s\bar{s}$  and  $c\bar{u} \rightarrow d\bar{d}$  [47–49]. If confirmed, large rescattering effects could also explain the large  $SU(3)_F$  breaking, order of 30%, that is observed in some branching fractions — for example, in the ratio  $\mathcal{B}(D^0 \rightarrow K^+ K^-)/\mathcal{B}(D^0 \rightarrow \pi^+ \pi^-)$  and in the relatively large value of  $\mathcal{B}(D^0 \rightarrow K_S^0 K_S^0)$  [44]. Improving our understanding of these nonperturbative effects, for example, through studies of the resonances that might contribute to rescattering [50], or through precise measurements of rescattering close to the mass scale of charmed hadrons [46], is crucial to provide precise predictions of  $CP$  asymmetries.

Nevertheless, it is already possible to relate the size of  $CP$  asymmetries of different decay channels through  $SU(3)_F$  or isospin symmetry arguments, which may be violated by BSM interactions [51–53]. For example, eq. (2.5) implies that in the limit of  $SU(3)_F$  symmetry the  $CP$  asymmetries for two decay channels related by a  $U$ -spin transformation,



such as  $D^0 \rightarrow K^+K^-$  and  $D^0 \rightarrow \pi^+\pi^-$ , have equal magnitude but opposite sign. Further examples will be provided in section 4.3.

### 3 The LHCb detector and charm physics

As both  $D^0$  oscillations and  $CP$  violation in charmed hadrons are effects of the order of  $10^{-3}$  or smaller, they require the collection of ten million decays or more to be observed. While samples of this size have first been collected at the  $B$  factories and by the CDF experiment, the last decade has witnessed a further leap forward in precision thanks to the start of operations of the LHCb experiment, which benefits from the high luminosity and huge production cross-section of charmed hadrons at the Large Hadron Collider [54, 55] as well as from a detector design dedicated to the study of heavy-quark hadrons.

The LHCb detector [56, 57] is a single-arm forward spectrometer covering the pseudorapidity range  $2 < \eta < 5$ , where the production of heavy quarks is concentrated [58]. It has recently been upgraded for *Run 3* of the LHC [59, 60]. The following description is of the experiment that operated during *Run 1* and 2. The tracking system consists of a silicon-strip vertex detector surrounding the proton-proton ( $pp$ ) interaction region, a large-area silicon-strip detector located upstream of a vertical dipole magnet with a bending power of about 4 Tm, and three stations of silicon-strip detectors and straw drift tubes placed downstream of the magnet. The minimum distance of a track to a primary  $pp$  collision vertex (PV), the impact parameter (IP), is measured with a resolution of  $(15 + 29/p_T) \mu\text{m}$ , where  $p_T$  is the component of the momentum transverse to the beam, in GeV/ $c$ . This exquisite performance is crucial for triggering on the displaced decay vertices of heavy-quark hadrons, rejecting the huge background of tracks originating in the PV. The momentum of charged particles is measured with a relative uncertainty which varies from 0.5% at low momentum to 1.0% at 200 GeV/ $c$ , guaranteeing a mass resolution of the order of 8 MeV/ $c^2$  for charmed-hadron decays into charged hadrons. Together with the particle identification capabilities ensured by a system of two ring-imaging Cherenkov detectors, this resolution ensures an excellent signal-to-background ratio for most of the decays of interest. Finally, the particle identification capabilities are complemented by a scintillating-pad and preshower detectors to distinguish photons and electrons, an electromagnetic and a hadronic calorimeter, and a muon detector composed of alternating layers of iron and multiwire proportional chambers.

The data sample collected to date corresponds to  $1(2) \text{ fb}^{-1}$  of integrated luminosity of  $pp$  collisions at a centre-of-mass energy of 7(8) TeV accumulated during the LHC *Run 1* (2011–2012), and to  $6 \text{ fb}^{-1}$  at 13 TeV accumulated during *Run 2* (2015–2018). The on-line event selection is performed by a hardware trigger, based on information from the calorimeter and muon systems, followed by a software trigger, which applies a full event reconstruction in two stages. Because of the large production rate of charm decays in the LHCb acceptance, of the order of 1 MHz [61, 62], the amount of data that can be written to permanent storage is one of the factors that limit the number of decays that can be collected. To mitigate this problem, since 2015 the alignment and calibration of the detector is performed in near real-time after the first stage of the software trigger [63].



The results are then used in the second stage, ensuring offline data quality already at the trigger level. This opens up the possibility to perform physics analyses directly using candidates reconstructed in the trigger, allowing only the triggered candidates to be stored to disk [64, 65]. The consequent reduction in the event size by one order of magnitude allows the rate at which data are collected to be increased, by loosening the trigger requirements. This accounts for a large part of the increased yield of charmed hadrons at equal luminosity achieved during *Run 2* compared to *Run 1*. Further gains are due to the higher charm production cross-section at larger centre-of-mass energy [54, 55] and to the introduction of a new two-track line looking for displaced vertices at the first stage of the software trigger, which complements the single-track line looking for tracks with high momentum and IP used during *Run 1*.

It should be emphasised that the collected yield of charmed hadrons, which are hereafter denoted as  $D$ , depends critically on their decay topology and on the trigger requirements. Contrary to charm and  $B$  factories, tight selections on the momentum and IP of the final-state particles as well as on the  $D$  flight distance are needed to distinguish the signal from the background of random combinations of light hadrons produced in the  $pp$  collision. Moreover, the first-stage software trigger is optimised for collecting  $B$  rather than  $D$  hadrons, and  $B$  hadrons are characterised by larger momentum and longer flight distance on average. This often constitutes the bottleneck for the charm collection efficiency, which can be much smaller than unity especially at low decay times and for multibody final states, where the momentum and IP of the final-state particles are smaller on average than those of two-body decays. For multibody decays, requirements on these variables can also provoke undesirable variations of the efficiency across the final-state phase space. The efficiency is even smaller for final states including  $K_S^0$  mesons and hyperons, which often decay outside of the vertex tracker or even after the tracker upstream of the magnet. Therefore, they are not reconstructed in the first-stage software trigger, which only relies on tracks producing a signal in the vertex tracker, or in the second case they are excluded also from the offline reconstruction as their momentum cannot be accurately measured. Even lower efficiencies are achieved for neutral pions since, even when the two photons in which they decay can be distinguished in the calorimeter, the  $\pi^0$  mass resolution is limited to approximately  $9 \text{ MeV}/c^2$ ; besides, the neutral pion cannot be associated to a single decay vertex. Tight momentum requirements are thus needed to minimise the combinatorial background [57, 66]. Finally, decay channels with a single  $K_L^0$  meson or neutrino could be reconstructed with approximate methods [67], but the unknown initial state of the  $D$  hadron poses additional challenges to the separation from background with respect to charm and  $B$  factories. No measurements of these decays have been published to date.

### 3.1 Measuring $CP$ asymmetries

The most common observable employed to search for  $CP$  violation is the time-dependent asymmetry between the decay widths of  $D \rightarrow f$  and  $\bar{D} \rightarrow \bar{f}$  decays,

$$A_{CP}(f, t) \equiv \frac{\Gamma(D \rightarrow f, t) - \Gamma(\bar{D} \rightarrow \bar{f}, t)}{\Gamma(D \rightarrow f, t) + \Gamma(\bar{D} \rightarrow \bar{f}, t)}, \quad (3.1)$$

where  $D$  denotes a charmed hadron, and  $t$  denotes its proper decay time. In the case of charged mesons,  $D^+$  or  $D_s^+$ , of baryons, or when the time-dependent contribution is irrelevant to the final result, all the quantities in eq. (3.1) are integrated over decay time.

This asymmetry is measured starting from the raw asymmetry between the yields of  $D$  and  $\bar{D}$  decays at decay time  $t$ . However, this encompasses additional contributions, which will globally be referred to as “nuisance asymmetries”, as follows,

$$A_{\text{raw}}(f, t) \approx A_{CP}(f, t) + A_{\text{det}}(f) + A_{\text{prod}}(D), \quad (3.2)$$

where  $A_{\text{det}}(f)$  is the detection asymmetry of the final state,  $A_{\text{prod}}(D)$  is the production asymmetry of  $D$  hadrons, and terms of third order in the asymmetries are neglected. Detection asymmetries arise from the interplay of several factors. For a given magnet polarity, low-momentum particles of one charge at large or small emission angles in the horizontal plane may be deflected out of the detector or into the uninstrumented beam pipe, whereas particles with the opposite charge are more likely to remain within the acceptance. This effect is cancelled to a large extent by periodically reversing the polarity of the magnet. Smaller residual asymmetries remaining after the averaging are due to right-left misalignment of detector elements and to the small shift of the collision point with respect to the symmetry axis of the detector; to different beam-beam crossing angles for opposite magnet polarities; and to variations of the detection efficiency over time. The different interaction cross-section of positively and negatively charged kaons and pions with matter plays a role as well, especially when the selection at the hardware-trigger level is based on the information from the hadronic calorimeter. On the other hand, the production asymmetry is due to the asymmetric hadronisation of  $c\bar{c}$  pairs into the different species of charmed hadrons and anti-hadrons, since the  $pp$  initial state is not self-conjugate.

Nuisance asymmetries are not reproduced by simulation with the required level of precision, and must be corrected for through methods based on collected data. This is usually done by measuring the difference between the raw asymmetry of the SCS of interest with one or more CF decays which share the same nuisance asymmetries, but the dynamical asymmetries of which are expected to be negligible; or with SCS decays whose  $CP$  asymmetry is known with better precision.

Finally, when analysing decays into a final state that is shared by  $D^0$  and  $\bar{D}^0$  mesons, their initial flavour can be identified only through their production mechanism. This is done by measuring the charge of the accompanying particle in strong  $D^*(2010)^+ \rightarrow D^0\pi^+$  decays or in inclusive  $B \rightarrow \bar{D}^0\mu^+X$  decays, where  $B$  stands for a  $b$  hadron and  $X$  for an arbitrary set of unreconstructed particles. Hereafter the  $D^*(2010)^+$  meson is referred to as  $D^{*+}$ , and the two tagging categories as  $D^{*+}$ -tagged and  $\mu^-$ -tagged decays. Both categories introduce a further detection asymmetry due to the tagging particle,  $\pi^+$  or  $\mu^-$ , in eq. (3.2). This asymmetry is corrected for in the same way as the others. The  $D^{*+}$ -tagged sample is larger by around a factor of three and is purer, thanks to the larger production cross-section of charm with respect to beauty hadrons and to the low  $Q$  value<sup>6</sup> of the  $D^{*+}$  decay. The low  $Q$

---

<sup>6</sup>The  $Q$  value of a decay is defined as the energy released in the decay, and is equal to the mass of the decaying particle minus the sum of the masses of its decay products.

value ensures excellent mass resolution for the  $D^{*+}$  meson, and causes the pion momentum to form a very small angle with that of the  $D^0$  meson, thus reducing the combinatorial background. On the other hand, this small angle implies a poor resolution on the  $D^{*+}$  decay vertex, which is therefore constrained to originate in the PV to achieve the best possible resolutions on the  $D^{*+}$  mass, around  $0.5 \text{ MeV}/c^2$ , and on the  $D^0$  decay time [68]. The resolution on decay time, approximately 40 ps, corresponds to around 0.1  $D^0$  lifetimes and is a factor of three better than that of the  $\mu^-$ -tagged sample. However, the constraint biases the measured decay time of  $D^0$  from secondary  $D^{*+}$  mesons that are produced in  $B$  decays to larger values. Therefore, secondary mesons are treated as a background in most measurements. This background can be troublesome, as the production asymmetry of secondary mesons differs from that of the prompt ones; moreover, their fraction increases with decay time. On the other hand,  $\mu^-$ -tagged candidates benefit from looser trigger requirements, allowing a larger reconstruction efficiency at low  $D^0$  decay times as well as a flatter efficiency across the final-state phase space in multibody decays to be obtained, although at the cost of increased background. This background can be reduced by using doubly tagged  $B \rightarrow D^{*-}(\rightarrow \bar{D}^0\pi^-)\mu^+X$  decays, but the resulting yield is considerably smaller.

## 4 Searches for $CP$ violation in the decay

The next sections review the most recent LHCb searches for  $CP$  violation in the decay, starting from the historic first observation of  $CP$  violation achieved in 2019.

### 4.1 Observation of $CP$ violation in $D^0 \rightarrow h^+h^-$ decays

$CP$  violation was observed for the first time in charm decays by the LHCb collaboration in 2019, through a measurement of the difference between the time-integrated  $CP$  asymmetries of  $D^0 \rightarrow K^+K^-$  and  $D^0 \rightarrow \pi^+\pi^-$  decays,  $\Delta A_{CP}$  [69, 70]. This is a very convenient observable, since nuisance asymmetries cancel in the difference, whereas the  $CP$  asymmetries in the decay are expected to have opposite signs and their magnitudes add up; see eq. (2.5). The contribution to  $\Delta A_{CP}$  from time-dependent  $CP$  violation also tends to cancel in the difference, as the time-dependent asymmetry of the  $D^0$  and  $\bar{D}^0$  decay rates into a  $CP$ -even final state  $f$  is equal to

$$A_{CP}(f, t) \equiv \frac{\Gamma(D^0 \rightarrow f, t) - \Gamma(\bar{D}^0 \rightarrow f, t)}{\Gamma(D^0 \rightarrow f, t) + \Gamma(\bar{D}^0 \rightarrow f, t)} \approx a_f^d + \Delta Y_f \frac{t}{\tau_{D^0}}, \quad (4.1)$$

where terms of order higher than two in the mixing parameters are neglected,  $a_f^d$  is the  $CP$  asymmetry in the decay,  $\tau_{D^0}$  is the  $D^0$  lifetime, and the expression of the parameter  $\Delta Y_f$  in terms of the theoretical mixing parameters is given in section 5.1.<sup>7</sup> The time-integrated  $CP$  asymmetry is therefore equal to

$$A_{CP}(f) \approx a_f^d + \Delta Y_f \frac{\langle t \rangle_f}{\tau_{D^0}}, \quad (4.2)$$

---

<sup>7</sup>The parameter  $\Delta Y_f$  is equal to the negative of the parameter  $A_f^d$  sometimes used in the literature, defined as the asymmetry of the effective decay widths of  $D^0$  and  $\bar{D}^0$  mesons into the final state  $f$ , up to a multiplicative factor which differs from unity by less than 1% [71, 72].

where  $\langle t \rangle_f$  is the average decay time of the analysed sample, and depends on the selection requirements. Assuming that  $\Delta Y_f$  is independent of the final state, see section 5.1, and denoting it with  $\Delta Y$ , the following relation holds,

$$\Delta A_{CP} \approx a_{K^+K^-}^d - a_{\pi^+\pi^-}^d + \Delta Y \frac{\langle t \rangle_{K^+K^-} - \langle t \rangle_{\pi^+\pi^-}}{\tau_{D^0}}. \quad (4.3)$$

The contribution to  $\Delta A_{CP}$  from time-dependent  $CP$  violation is very small, since the average decay times of the selected samples of  $D^0 \rightarrow K^+K^-$  and  $D^0 \rightarrow \pi^+\pi^-$  decays differ by less than  $0.15 \tau_{D^0}$ , and  $\Delta Y$  is measured to be consistent with zero with a precision close to  $10^{-4}$  [71, 73–75].

The observation of  $CP$  violation is based on the *Run 2* data sample, including both  $D^{*+}$  and  $\mu^-$  tagged candidates, which corresponds to around 53 million  $D^0 \rightarrow K^+K^-$  and 17 million  $D^0 \rightarrow \pi^+\pi^-$  decays. The mass distributions of the  $D^{*+}$ -tagged candidates, which constitute the vast majority of the sample, are shown in fig. 3. The result is

$$\Delta A_{CP} = (-1.82 \pm 0.32 \pm 0.09) \times 10^{-3},$$

where the systematic uncertainty is significantly smaller than the statistical one, thanks to the cancellation of most systematic effects in the difference, and is expected to be reducible when larger samples will become available. A combination with the result of the  $\mu^-$ -tagged sample and with previous determinations [76, 77], including a small correction for a residual contribution from time-dependent  $CP$  violation [73–75], see eq. (4.3), yields

$$a_{K^+K^-}^d - a_{\pi^+\pi^-}^d = (-1.57 \pm 0.29) \times 10^{-3},$$

which is inconsistent with the hypothesis of  $CP$  symmetry at the level of 5.3 standard deviations.

This value is larger by a factor of five than perturbative estimates [14, 33, 78, 79] and predictions from light-cone sum rules [23, 80]. While its unexpectedly large size has prompted several BSM interpretations [23, 81, 82], other authors have claimed that it can be explained within the SM through a mild nonperturbative enhancement of  $A_b$  due to final-state interactions [46, 78, 83]. Explicit models of such an enhancement, which may also explain the factor-of-three difference between the branching fractions of  $D^0 \rightarrow K^+K^-$  and  $D^0 \rightarrow \pi^+\pi^-$  decays without invoking large  $U$ -spin breaking effects [44], have been proposed in refs. [50, 84].

Progress of *ab initio* theoretical predictions is ultimately needed to rigorously assess the compatibility of the measurement with the SM. Meanwhile, additional measurements of  $CP$  asymmetries and of poorly known branching fractions of other decay channels, as well as of the scalar resonances that might be responsible for rescattering,<sup>8</sup> would constitute an

---

<sup>8</sup>For example, it would be important to measure the branching fractions of the  $f_0(1710)$  and  $f_0(1790)$  resonances into the  $\pi^+\pi^-$  and  $K^+K^-$  final states [50]. In addition, if large rescattering through these resonances is responsible for the enhancement of the  $CP$  asymmetries of  $D^0 \rightarrow K^+K^-$  and  $D^0 \rightarrow \pi^+\pi^-$  decays, the same mechanism could enhance also other observables like the branching fraction of  $D^0 \rightarrow \gamma\gamma$  decays [85–87].

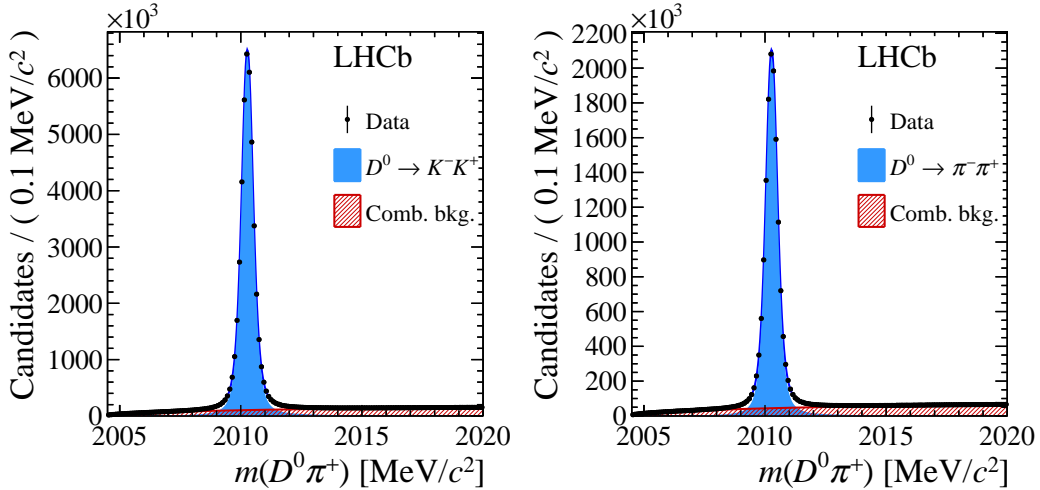


**Figure 3.** Invariant-mass distribution of the  $D^{*+}$  candidates yielding the first observation of  $CP$  violation in charm decays in the (left)  $D^0 \rightarrow K^+K^-$  and (right)  $D^0 \rightarrow \pi^+\pi^-$  final states. The  $\mu^-$ -tagged sample is considerably smaller. Figures taken from ref. [69].

invaluable tool to pin down the nature of the nonperturbative effects at play, and to test available models [50, 83, 88, 89].<sup>9</sup>

In particular, an individual measurement of  $a_{K^+K^-}^d$  or  $a_{\pi^+\pi^-}^d$  would provide useful information on the size of  $U$ -spin breaking in  $A_b$ . Since their difference is already measured through the  $\Delta A_{CP}$  observable, only  $A_{CP}(K^+K^-)$  is directly measured and  $A_{CP}(\pi^+\pi^-)$  is derived indirectly. Measuring both asymmetries individually would not make an improvement, because their precision is limited by the correction for production and detection asymmetries, which would be the same for both decay channels (whereas such a correction is not needed for the measurement of  $\Delta A_{CP}$ ).

A very recent measurement determines  $A_{CP}(K^+K^-)$  using the *Run 2*  $D^{*+}$ -tagged data sample [100, 101]. The correction for the nuisance asymmetries relies on multiple subtractions of raw asymmetries using the following CF decay channels,

$$A_{CP}(K^+K^-) \approx A_{\text{raw}}(D^0 \rightarrow K^+K^-) - A_{\text{raw}}(D^0 \rightarrow K^-\pi^+) + A_{\text{raw}}(D^+ \rightarrow K^-\pi^+\pi^+) - A_{\text{raw}}(D^+ \rightarrow K_S^0\pi^+) + A_{\text{det}}(K^0), \quad (4.4)$$

or

$$A_{CP}(K^+K^-) \approx A_{\text{raw}}(D^0 \rightarrow K^+K^-) - A_{\text{raw}}(D^0 \rightarrow K^-\pi^+) + A_{\text{raw}}(D_s^+ \rightarrow K^-K^+\pi^+) - A_{\text{raw}}(D_s^+ \rightarrow K_S^0K^+) + A_{\text{det}}(K^0), \quad (4.5)$$

where the detection asymmetry of the neutral kaon includes a contribution from  $CP$  violation in  $K^0$  mixing and is calculated explicitly [102, 103]. The method based on eq. (4.5)

<sup>9</sup>Note, however, that global fits to charm branching ratios and  $CP$  asymmetries [45, 83, 88–95] are not necessarily able to distinguish the cases where  $CP$  violation originates from the SM or requires the presence of BSM interactions, and the validity of the assumptions of some of these fits has recently been challenged [96–99].

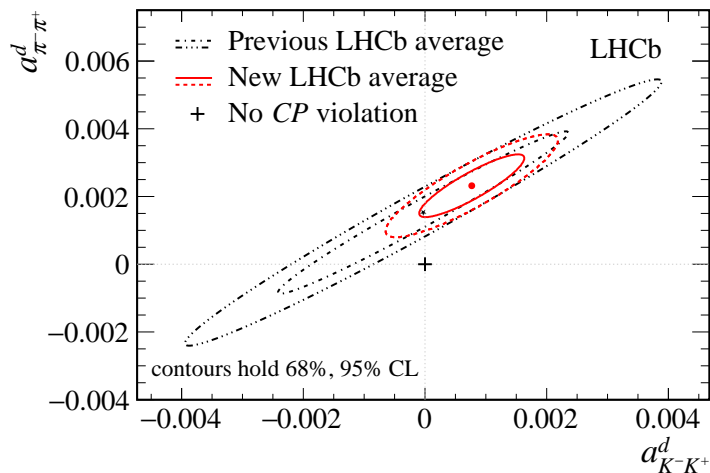


**Figure 4.** Best-fit values and two-dimensional confidence regions in the  $(a_{K^+K^-}^d, a_{\pi^+\pi^-}^d)$  plane for the combinations of the LHCb results obtained with the new  $A_{CP}(K^+K^-)$  measurement and without. Figure taken from ref. [100].

had never been used before, and allows the statistical uncertainty to be improved by 37% at equal integrated luminosity. In fact, for both methods, before measuring the raw asymmetries, the momentum distributions of the  $D$  mesons and of the final-state particles must be aligned by assigning per-candidate weights. This ensures a proper cancellation of the nuisance asymmetries, which depend on kinematics. However, due to the different topologies and number of final-state particles of these decays, the statistical uncertainty is significantly degraded by the weighting and is eventually limited by the  $D^+ \rightarrow K_S^0 \pi^+$  or  $D_s^+ \rightarrow K_S^0 K^+$  channels. Adding the new decay chain in eq. (4.5) thus allows the statistical uncertainty to be significantly reduced even at equal  $D^0 \rightarrow K^+K^-$  yield.

The average of the results obtained with the methods in eqs. (4.4) and (4.5) is

$$A_{CP}(D^0 \rightarrow K^+K^-) = (6.8 \pm 5.4 \pm 1.6) \times 10^{-4},$$

where the systematic uncertainty is, again, limited by the size of the calibration samples and could in principle be reduced as their size increases. Contrary to  $\Delta A_{CP}$ , in this case the contribution from time-dependent  $CP$  violation in eq. (4.2) cannot be neglected, as the average decay time of the collected  $D^0 \rightarrow K^+K^-$  decays is approximately equal to  $1.7 \tau_{D^0}$ . Therefore, the result is combined with previous determinations of  $A_{CP}(K^+K^-)$  [76, 104],  $\Delta A_{CP}$  [69, 76, 77] and  $\Delta Y$  [71, 73–75] to determine the  $CP$  asymmetries in the decay  $a_{K^+K^-}^d$  and  $a_{\pi^+\pi^-}^d$ ; see fig. 4. The numerical results are

$$\begin{aligned} a_{K^+K^-}^d &= (7.7 \pm 5.7) \times 10^{-4}, \\ a_{\pi^+\pi^-}^d &= (23.2 \pm 6.1) \times 10^{-4}, \end{aligned}$$

where the uncertainties include systematic and statistical contributions and the correlation coefficient is equal to 0.88. The results are consistent with the SM expectations for the

size of  $U$ -spin breaking [46, 83, 84, 105], and the second shows a departure from zero at the level of 3.8 standard deviations.

Larger data samples from *Run 3* and beyond are needed to establish a first observation of  $CP$  violation in either of the two individual decay channels, and to assess the level of  $U$ -spin breaking in  $A_b$ . In the mean time, measurements of other decay channels can provide complementary information on the origin of  $CP$  violation in charm, as discussed in the next sections.

## 4.2 Search for $CP$ violation in $D^0 \rightarrow K_S^0 K_S^0$ decays

The size of  $CP$  violation could be larger in  $D^0 \rightarrow K_S^0 K_S^0$  decays, where only exchange and penguin-annihilation diagrams that vanish in the  $U$ -spin limit contribute to  $A_{sd}$ , while the  $CP$ -violating contributions to  $A_b$  from the same diagrams do not cancel out. Therefore, the  $CP$  asymmetry in the decay might be as large as 1% [47, 48], even if somewhat smaller values are favoured by most models [83, 88, 89].

The LHCb collaboration has recently measured the time-integrated  $CP$  asymmetry of this decay mode employing the *Run 2*  $D^{*+}$ -tagged data sample [106, 107]. The  $K_S^0$  candidates are reconstructed in the  $\pi^+\pi^-$  final state, either from tracks that generated signals in all the tracking stations including the vertex detector (if the  $K_S^0$  meson decayed early enough), or otherwise from the two trackers immediately upstream and downstream of the magnet only. The two categories are named *long* and *downstream* and are labelled “L” and “D”, respectively. The  $D^0$  candidates are classified accordingly into three categories: LL, LD and DD. Downstream  $K_S^0$  candidates have a geometrical acceptance larger than that of long candidates by a factor of two, but they are not selected by the first-stage software trigger. As a consequence, DD candidates are selected only if the first-stage trigger has been activated by unrelated tracks in the event, and they are fewer than LL and LD candidates. Moreover, the  $D^0$ -mass and decay-vertex resolutions are degraded for candidates containing downstream kaons. This reduces the capability to distinguish prompt mesons from secondary mesons. Therefore, contrary to most charm measurements, no requirements are applied to reject the latter category.

To maximise the statistical precision, the total sample is further subdivided into nine categories, based on the compatibility of the  $D^0$  candidate with originating from the PV, and on the output of a multivariate classifier trained to reject combinatorial background. This allows some categories to benefit from a better signal-to-background ratio; see fig. 5. The nuisance asymmetries are removed by subtraction with the raw asymmetry of  $D^0 \rightarrow K^+K^-$  decays, weighting each  $D^0$  candidate with momentum  $\vec{p}$  by

$$w^\pm(\vec{p}) = \frac{n_{K^+K^-}^+(\vec{p}) + n_{K^+K^-}^-(\vec{p})}{2n_{K^+K^-}^\pm(\vec{p})} [1 \pm A_{CP}(D^0 \rightarrow K^+K^-)], \quad (4.6)$$

where the plus (minus) sign applies to  $D^0$  ( $\bar{D}^0$ ) candidates and  $n_{K^+K^-}^\pm(\vec{p})$  is the local density of  $D^0$  ( $\bar{D}^0$ ) mesons with momentum  $\vec{p}$  decaying into the  $K^+K^-$  final state, as estimated with a multivariate classifier. The selection requirements of the signal and control samples are aligned to ensure an effective cancellation of the detection asymmetry of the tagging pion and of the production asymmetries of prompt and secondary  $D^{*+}$  mesons.



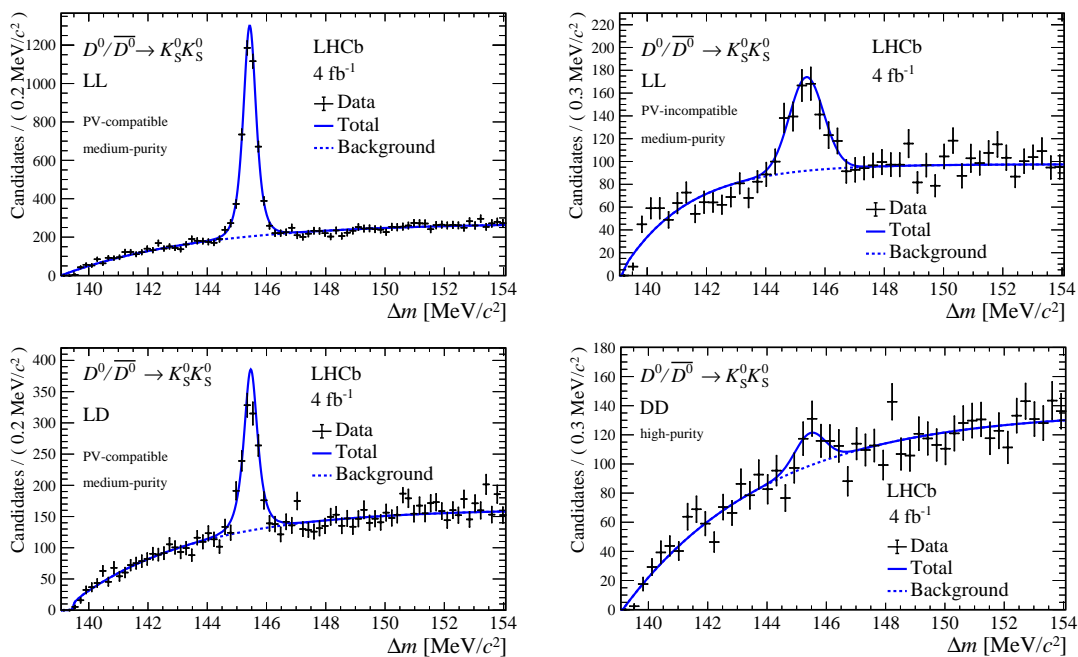


**Figure 5.** Distribution of the difference of the  $D^{*+}$  and  $D^0$  invariant masses, for the most significant  $D^0 \rightarrow K_S^0 K_S^0$  categories. Fit projections are overlaid. Figure taken from ref. [106].

Finally, the asymmetry is measured through a simultaneous fit to the weighted distributions of the invariant masses of the two  $K_S^0$  mesons and to the difference of the invariant masses of the  $D^{*+}$  and  $D^0$  mesons. The results for the nine categories are compatible with each other, and are combined to yield

$$A_{CP}(D^0 \rightarrow K_S^0 K_S^0) = (-3.1 \pm 1.2 \pm 0.4 \pm 0.2)\%,$$

where the third uncertainty is due to the precision with which the  $CP$  asymmetry of the control channel is known [104], and the systematic uncertainty is dominated by the uncertainty on the shape of the mass distributions and by the statistical uncertainty on the weighting, which are both expected to decrease with future larger data samples. This result supersedes that of ref. [108] and is compatible, but more precise, than previous determinations [109–111]. The new world average,  $A_{CP}(D^0 \rightarrow K_S^0 K_S^0) = (-1.9 \pm 1.0)\%$ , is compatible with the absence of  $CP$  violation within 1.9 standard deviations, with a precision equal to the upper edge of the SM predictions.

### 4.3 Search for $CP$ violation in $D_{(s)}^+ \rightarrow h^0 h^+$ decays

While predicting the absolute size of  $CP$  violation in charm in the SM is a formidable challenge, one can easily derive  $SU(3)_F$ -based sum rules relating its size in different decay channels [51–53, 112]. These rules might be violated by new interactions beyond the level expected in the SM, where the size of  $SU(3)_F$  breaking is around 30% [23, 44]. Another testable feature of the SM is that QCD penguin diagrams contribute only to  $\Delta I = 1/2$  transitions, whereas  $\Delta I = 3/2$  transitions are allowed only at tree-level and

therefore cannot give rise to  $CP$  violation [51]. By measuring the branching ratios and  $CP$  asymmetries of decays sharing the same isospin amplitudes, such as  $D^0 \rightarrow \pi^+\pi^-$  and  $D^0 \rightarrow \pi^0\pi^0$ , one can determine whether the individual  $CP$  asymmetries can be interpreted only in terms of  $\Delta I = 1/2$  amplitudes, or if they require the presence of  $\Delta I = 3/2$  contributions from BSM interactions. The  $D^+ \rightarrow \pi^+\pi^0$  decay is particularly interesting as its  $CP$  asymmetry is expected to be smaller than  $10^{-5}$ , even if it is SCS, since it is a pure  $\Delta I = 3/2$  transition. Unfortunately, the precision of all these tests is limited by decay channels involving neutral particles, which are reconstructed with low efficiency at hadron colliders.

The LHCb collaboration has recently measured the  $CP$  asymmetries of  $D_{(s)}^+ \rightarrow h^+h^0$  decays, where  $h^+$  stands for a  $\pi^+$  or  $K^+$  meson, and  $h^0$  for a  $\pi^0$ ,  $\eta$  or  $\eta'$  meson, with the data sample collected in *Run 1* and *2* [113, 114]. For the first time,  $\pi^0$  and  $\eta$  mesons are reconstructed through Dalitz decays,  $h^0 \rightarrow e^+e^-\gamma$ , or two-photon decays where one of the photons converts into an electron-positron pair within the vertex detector. The latter sample is larger by a factor of six. Both decay chains allow triggering on the displaced  $D$ -meson decay vertex, which would be impossible to reconstruct using bare two-photon decays. While these decay chains account for only a small fraction of the total decays, this suppression is counterbalanced by the large charmed-hadron production cross-section with respect to  $B$  factories, which allows for results to be obtained that are equally or more precise. On the other hand, the signal-to-background ratio is lower than in other hadronic charm decays, and the measurement requires a careful correction for electron and positron bremsstrahlung in the magnetic field. For  $h^+$  equal to  $\pi^+$ , the  $\eta$  mesons are additionally reconstructed in the  $\gamma\pi^+\pi^-$  final state, achieving a similar precision. The same final state is used for the  $\eta'$  in  $D_{(s)}^+ \rightarrow \eta'\pi^+$  decays, too.

For all final states, the  $CP$  asymmetries are measured from a two-dimensional fit to the invariant mass distributions of the  $D_{(s)}^+$  and  $h^0$  candidates, where the probability distributions are based on simulation and account for correlations, especially between the radiative tails. The fit projections are shown in fig. 6. Detection asymmetries are removed by subtraction with  $D_{(s)}^+ \rightarrow h^+K_S^0$  or  $D_{(s)}^+ \rightarrow h^+\phi$  calibration decays, the kinematics of which is weighted to match that of the signal decays; the  $K_S^0$  detection asymmetry is corrected for with an explicit calculation [102]. The results are

$$\begin{aligned}
A_{CP}^{D^+ \rightarrow K^+\pi^0} &= (-3.2 \pm 4.7 \pm 2.1)\%, & A_{CP}^{D^+ \rightarrow K^+\eta} &= (-6 \pm 10 \pm 4)\%, \\
A_{CP}^{D^+ \rightarrow \pi^+\pi^0} &= (-1.3 \pm 0.9 \pm 0.6)\%, & A_{CP}^{D_s^+ \rightarrow K^+\pi^0} &= (-0.8 \pm 3.9 \pm 1.2)\%, \\
A_{CP}^{D^+ \rightarrow \pi^+\eta} &= (0.13 \pm 0.50 \pm 0.18)\%, & A_{CP}^{D_s^+ \rightarrow K^+\eta} &= (0.9 \pm 3.7 \pm 1.1)\%, \\
A_{CP}^{D^+ \rightarrow \pi^+\eta'} &= (0.43 \pm 0.17 \pm 0.10)\%, & &
\end{aligned}$$

where the first and the subsequent rows correspond to DCS and SCS decays, respectively, and the systematic uncertainties are mainly due to the uncertainty on the fit models. They are all consistent with the absence of  $CP$  violation and they are in agreement with previous determinations at  $B$  and charm factories [115–118], while their precision is comparable or better.

#### 4.4 Multibody decays

Even if the most precise searches for  $CP$  violation to date concern two-body and quasi-two body decays [69, 100, 119], an extensive set of searches in  $D$  multibody decays are also being pursued. Their rich resonant structure and the variations of the strong phases across their final-state phase space may provide further handles to pin down the size of nonperturbative QCD effects and to understand the nature of the interactions responsible for  $CP$  violation. Some of these decays, such as  $D^0 \rightarrow K_S^0 K^\pm \pi^\mp$ , could display enhanced  $CP$  asymmetries, thanks to a mechanism analogous to that described in section 4.2 [49].

A whole variety of model-independent methods [120–124] have been developed and used for the study of multibody decays during *Run 1* [66, 125–130] as an intermediate step towards amplitude analyses which would be crucial to theoretically interpret an observation of  $CP$  violation. Some efforts have been devoted also to amplitude analyses, either allowing for the presence of  $CP$  violation [131, 132] or not [133–135]. Many new measurements based on the *Run 2* sample, which guarantees much larger signal yields thanks to the improvements in triggering [65], are underway. Finally, a recent amplitude analysis of the  $\Lambda_c^+ \rightarrow p K^- \pi^+$  decay and of the  $\Lambda_c^+$  production polarisation in semimuonic  $B$  decays [136] paves the way to future measurements of its electric and magnetic dipole moments, which are sensitive to BSM interactions of the charm quark and to the QCD structure of the  $\Lambda_c^+$  baryon, respectively [137–141].

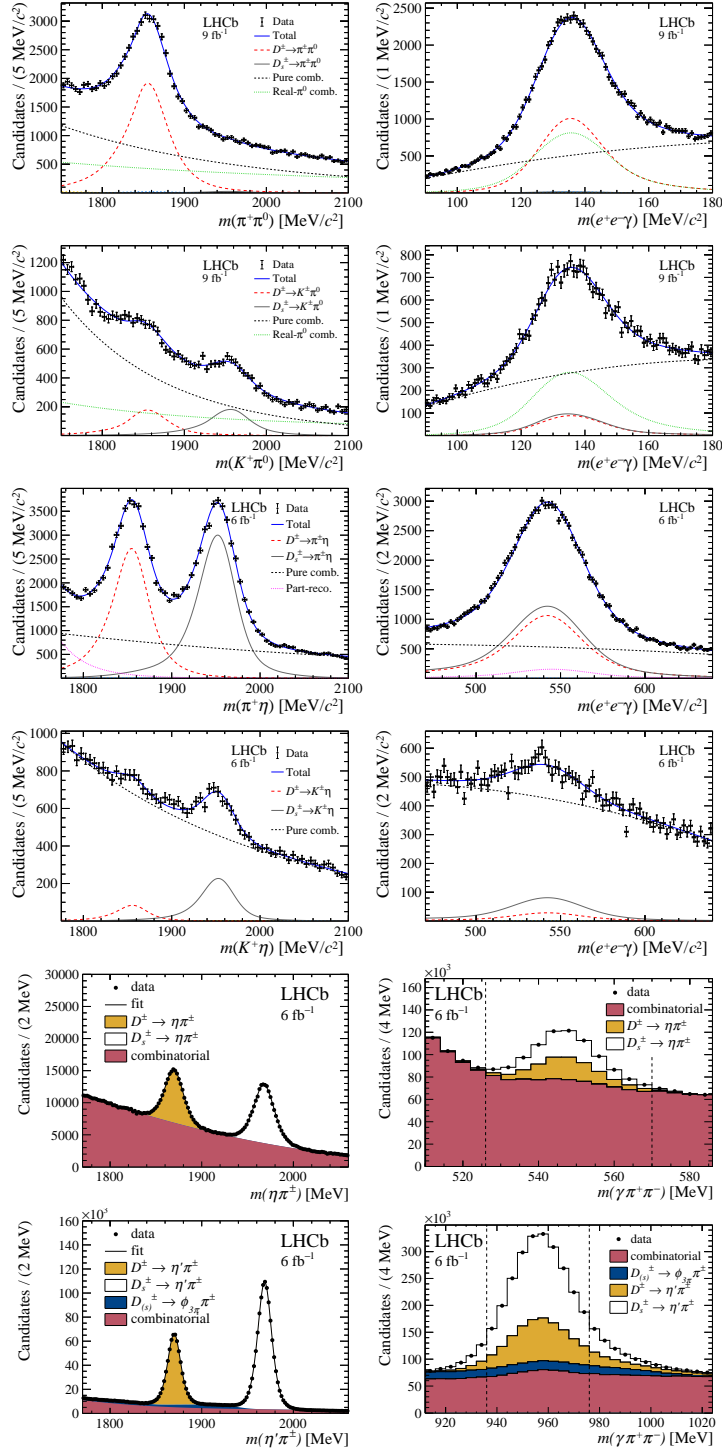


**Figure 6.** Distribution of (left)  $m(h^+h^0)$  and (right) the invariant mass of the corresponding neutral meson, for the various combinations of  $D_{(s)}^+$  decays analysed in refs. [113, 114], from which the figures are taken. Projections of the fit results and individual fit components are overlaid. In the right figures of the two bottom rows, the  $m(\gamma\pi^+\pi^-)$  mass range is enlarged with respect to the baseline fit, and the default mass range is indicated by the vertical dashed lines.

## 5 Time-dependent measurements

Searches for time-dependent  $CP$  violation are mostly sensitive to  $CP$  violation in the mixing amplitudes [21], and thus they are complementary to those of  $CP$  violation in the decay. However, they require even better experimental precision. In fact, in the SM the contribution of  $CP$  violation in the mixing to the  $CP$  asymmetries is typically suppressed by one order in the  $U$ -spin breaking parameter  $\epsilon$  with respect to that of  $CP$  violation in the decay [21]. While  $CP$  violation in the mixing has not been observed yet, the past two years have witnessed a leap forward in the precision of its search and of the measurements of the mixing parameters, as described in the next sections.

### 5.1 Search for time-dependent $CP$ violation in $D^0 \rightarrow h^+h^-$ decays

The  $CP$ -even, SCS final states  $f = K^+K^-$  or  $\pi^+\pi^-$  provide a clean way to measure the dispersive  $CP$ -violating contributions to  $D^0$  mixing. The relevant observable is the slope,  $\Delta Y_f$ , of the time-dependent asymmetry of the  $D^0$  and  $\bar{D}^0$  decay widths defined in eq. (4.1). This observable is approximately equal to [21]

$$\Delta Y_f \approx -x_{12} \sin \phi_2^M + y_{12} a_f^d \left( 1 + \frac{x_{12}}{y_{12}} \cot \delta_f \right), \quad (5.1)$$

where  $\delta_f$  is the strong-phase difference between  $A_b$  and  $A_{sd}$ . In the very long term, the dependence of  $\Delta Y_f$  on the final state could be used to measure  $\delta_f$ , using external inputs for the mixing parameters, weak phase  $\phi_2^M$  and  $a_f^d$  [21]. However, assuming that  $\delta_f$  is not fine-tuned to zero or  $\pi$  (as expected from large rescattering at the charm mass scale), final-state dependent contributions are of the order of  $10^{-5}$  [31, 69, 100] and can be neglected at the current level of experimental precision. The  $\Delta Y_f$  parameter is consequently assumed to be independent of the final state and is denoted as  $\Delta Y \equiv -x_{12} \sin \phi_2^M$ . Its value sets a direct constraint on the dispersive weak phase  $\phi_2^M$ , thanks to independent determinations of  $x_{12}$  [31]. Reducing the uncertainty on  $\Delta Y_f$  is essential not only to constrain possible  $CP$ -violating BSM interactions, but also to determine the parameter  $a_{K^+K^-}^d$  from the measurements of the time-integrated asymmetry of  $D^0 \rightarrow K^+K^-$  decays, as described in section 4.1.

The  $\Delta Y$  parameter has been recently measured using the  $D^{*+}$ -tagged data sample collected during *Run 2* [71, 142], which comprises 58 million and 18 million  $D^0 \rightarrow K^+K^-$  and  $D^0 \rightarrow \pi^+\pi^-$  decays, respectively. The main background, which comes from random associations of unrelated particles, is around 5% of the signal and is removed through a sideband subtraction in the  $m(D^0\pi_{\text{tag}}^+)$  variable.

While the measurement is insensitive by construction to time-independent asymmetries, a time dependence of the detection and production asymmetries is indirectly introduced by the trigger requirements, even if these nuisance asymmetries depend explicitly only on the particles momenta. In fact, requirements on displacement-related variables like the  $D^0$  flight distance and the IP of its daughter particles with respect to the PV select  $D^0$  mesons with low decay times only if their momentum is large enough. As a result, low decay times correspond on average to larger momenta, and momentum-dependent asymmetries give rise to artificial time-dependent asymmetries; see fig. 7. These effects are

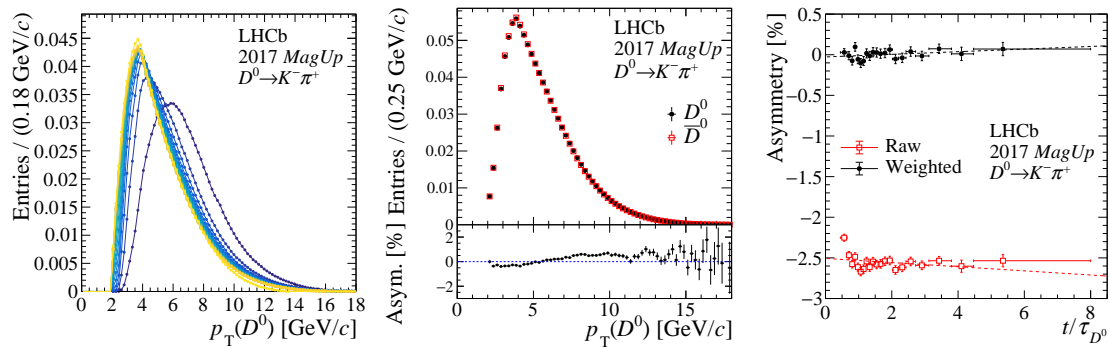


**Figure 7.** (Left) Normalised distributions of the  $D^0$  transverse momentum, in different colours for each decay-time interval in fig. 8. Decay time increases from blue to yellow colour. (Centre) Asymmetry between the normalised  $p_T$  distributions of  $D^0$  and  $\bar{D}^0$  mesons. (Right) Linear fit to the time-dependent asymmetry (red) before and (black) after the kinematic equalisation, after which the time-integrated asymmetry is zero by construction. All plots correspond to  $D^0 \rightarrow K^- \pi^+$  candidates collected in 2017 with the magnet polarity pointing upwards. Figures taken from ref. [71].

studied in a control sample of 518 million  $D^0 \rightarrow K^- \pi^+$  decays, for which the dynamical time-dependent asymmetry is known to be smaller than the experimental precision [71, 72]. The nuisance asymmetries are up to six times larger than the statistical uncertainty of the measurement, and are removed by equalising the vector-momentum distributions of the  $\pi_{\text{tag}}^+/\pi_{\text{tag}}^-$  and  $D^0/\bar{D}^0$  mesons through per-event weights. This removes by construction the dependence of the nuisance asymmetries on momentum and consequently on time; see fig. 7 right. While the equalisation marginally biases also the dynamical asymmetry, this effect is measured to be small and is corrected for. On the other hand, the equalisation allows to avoid the loss of statistical precision due to the weighting of multiple calibration channels that would otherwise be needed to correct for the nuisance asymmetries, as done in time-integrated measurements; see section 4.1. Naturally this procedure allows to measure only the time-dependent contribution of the asymmetry, and not the time-independent parameter  $a_f^d$ .

The production asymmetry of secondary mesons differs from that of prompt mesons, and their fraction increases with decay time. This background would thus bias the measurement even after the kinematic equalisation. Both the asymmetry and the fraction of secondary mesons are measured through a fit to the two-dimensional IP distribution of the  $D^0$  meson with respect to its PV, as a function of its decay time. Most of the secondary mesons are rejected by requiring the IP of the  $D^0$  meson to be greater than  $60 \mu\text{m}$ , and a correction of  $0.3 \times 10^{-4}$  is applied to the measurement of  $\Delta Y$  to account for their residual 4% contamination.

The analogue of  $\Delta Y$  for the control sample is measured from a binned linear fit to the time-dependent asymmetry of the  $D^0$  and  $\bar{D}^0$  weighted yields. The result, after the aforementioned correction for the bias from secondary mesons, is  $\Delta Y_{K^- \pi^+} = (-0.4 \pm 0.5 \pm 0.2) \times 10^{-4}$ , and is compatible with zero (as expected) within an uncertainty smaller than that of the final measurement by more than a factor of two. The linear fits to the

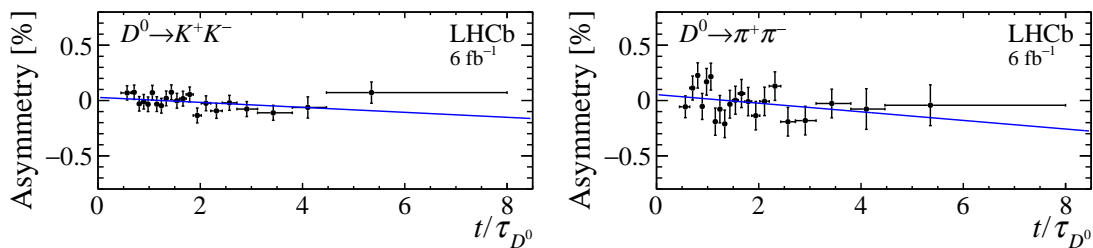


**Figure 8.** Asymmetry as a function of decay time for (left)  $D^0 \rightarrow K^+ K^-$  and (right)  $D^0 \rightarrow \pi^+ \pi^-$  candidates. A linear fit is superimposed. Figures taken from ref. [71].

time-dependent asymmetry for the signal samples are shown in fig. 8. The results,

$$\begin{aligned} \Delta Y_{K^+ K^-} &= (-2.3 \pm 1.5 \pm 0.3) \times 10^{-4}, \\ \Delta Y_{\pi^+ \pi^-} &= (-4.0 \pm 2.8 \pm 0.4) \times 10^{-4}, \end{aligned}$$

are compatible with the absence of  $CP$  violation at the level of two standard deviations and are in keeping with previous determinations [73–75, 143–145]. They constitute the most precise search for  $CP$  violation performed at a hadron collider to date and, neglecting possible differences between the  $K^+ K^-$  and  $\pi^+ \pi^-$  final states, they improve the precision of the previous world average by nearly a factor of two [146], yielding

$$\Delta Y = (-1.0 \pm 1.1 \pm 0.3) \times 10^{-4}.$$

The reduction of the systematic uncertainty by a factor of three with respect to the previous most precise determination [74], as well as the fact that it is dominated by the statistical precision with which the asymmetry of the combinatorial background is known and thus is expected to decrease as the size of the analysed sample increases, pave the way for even more precise future measurements.

## 5.2 Observation of a nonzero mass difference between the neutral charmed-meson mass eigenstates with $D^0 \rightarrow K_S^0 \pi^+ \pi^-$ decays

Contrary to two-body decays [71, 72, 147, 148], multibody  $D^0$  decays allow to measure simultaneously all mixing parameters and  $CP$ -violation phases, rather than a combination of these parameters. This is made possible by the variation of the strong phase across their final-state phase space, caused by their rich resonance structure. However, they imply the additional complication of a multi-dimensional analysis of the final-state phase space. Especially at hadron colliders, the selection efficiency varies significantly across the phase space due to tight trigger requirements, and this effect must be accounted for.

This problem can be mitigated by using model-independent analysis methods such as that proposed in ref. [149] for  $D^0 \rightarrow K_S^0 \pi^+ \pi^-$  decays. There, the Dalitz plot is divided into 8 regions symmetric with respect to its bisector (see fig. 9), each having an approximately constant strong-phase difference,  $\Delta\delta$ , between the decay amplitudes in the two halves of the plot. The ratios of the yields of the upper to the lower half are measured for each of the 8 regions, labelled “ $b$ ”, and in 13 intervals of decay time, labelled “ $j$ ”, separately for  $D^0$  and



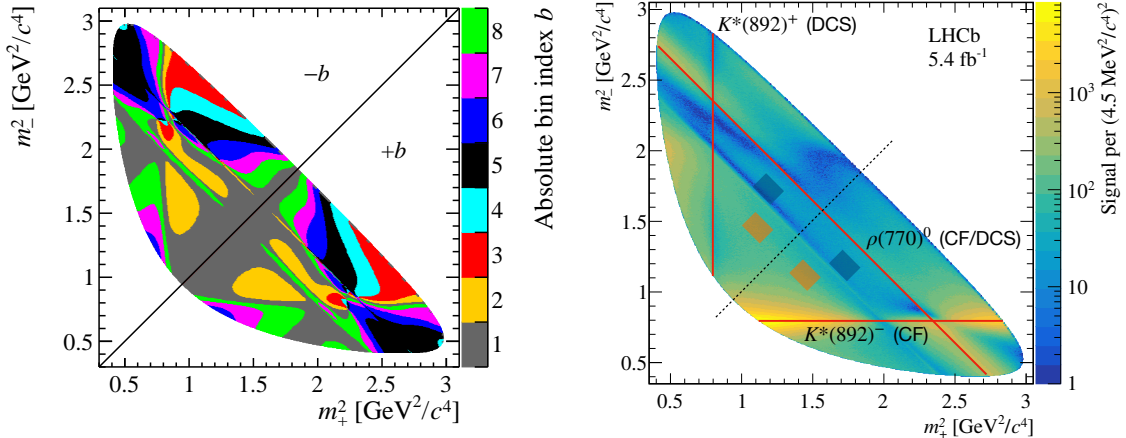


**Figure 9.** (Left) Iso- $\Delta\delta$  division of the Dalitz plot of  $D^0 \rightarrow K_S^0 \pi^+ \pi^-$  decays. The variable  $m_{\pm}$  is defined as  $m(K_S^0 \pi^{\pm})$  for  $D^0$  decays, and as  $m(K_S^0 \pi^{\mp})$  for  $\bar{D}^0$  decays. (Right) Dalitz plot of background-subtracted  $D^0 \rightarrow K_S^0 \pi^+ \pi^-$  candidates. The masses of the most relevant resonances are highlighted by the red lines. The coloured rectangles are an example of the regions used to decorrelate the  $D^0$  decay time and  $m(\pi^+ \pi^-)$  — note that the size and position of the rectangles used in the actual measurement are different. Figures adapted from refs. [150, 151].

$\bar{D}^0$  decays. Biases due to efficiency variations across the plot mostly cancel in the ratio, since the efficiency is approximately symmetric with respect to the bisector. A similar cancellation holds also for the production asymmetry and for the detection asymmetry of the tagging particle. On the other hand, the ratios provide nearly optimal sensitivity to the mixing parameters. In fact, the decays in the denominator mostly correspond to CF amplitudes and have nearly constant decay rates as a function of decay time, whereas the decay amplitudes in the numerator are mostly DCS, so that the fraction of CF decays following mixing is comparable in size and the decay rate significantly increases as a function of decay time. In particular, the ratios are equal to

$$R_{bj}^{\pm} \approx \frac{r_b + \sqrt{r_b} \operatorname{Re}[X_b^*(z_{CP} \pm \Delta z)] \langle t \rangle_j + \frac{1}{4} [|z_{CP} \pm \Delta z|^2 + r_b \operatorname{Re}(z_{CP}^2 - \Delta z^2)] \langle t^2 \rangle_j}{1 + \sqrt{r_b} \operatorname{Re}[X_b(z_{CP} \pm \Delta z)] \langle t \rangle_j + \frac{1}{4} [\operatorname{Re}(z_{CP}^2 - \Delta z^2) + r_b |z_{CP} \pm \Delta z|^2] \langle t^2 \rangle_j} \quad (5.2)$$

$$\approx r_b + \sqrt{r_b} [s_b(1 + r_b)(x_{CP} \pm \Delta x) - c_b(1 - r_b)(y_{CP} \pm \Delta y)] \langle t \rangle_j,$$

where the plus (minus) sign applies to the ratio of  $D^0$  ( $\bar{D}^0$ ) decays; the first and second line have been expanded up to second and to first order in the mixing parameters, respectively;  $r_b$  is the ratio at zero decay time;  $X_b \equiv c_b + i s_b$  is the average of  $e^{i\Delta\delta}$  in the region “ $b$ ”, as measured at charm factories [150, 152]; and the two complex parameters  $z_{CP} \equiv -(y_{CP} + i x_{CP})$  and  $\Delta z \equiv -(\Delta y + i \Delta x)$  are defined as

$$\begin{aligned} x_{CP} &\equiv x_{12} \cos \phi_2^M, & \Delta x &\equiv -y_{12} \sin \phi_2^\Gamma, \\ y_{CP} &\equiv y_{12} \cos \phi_2^\Gamma, & \Delta y &\equiv x_{12} \sin \phi_2^M = -\Delta Y. \end{aligned} \quad (5.3)$$

A new measurement [151] based on the  $D^{*+}$ -tagged data sample collected in *Run 2* increases the signal yield tenfold with respect to the previous determination based on

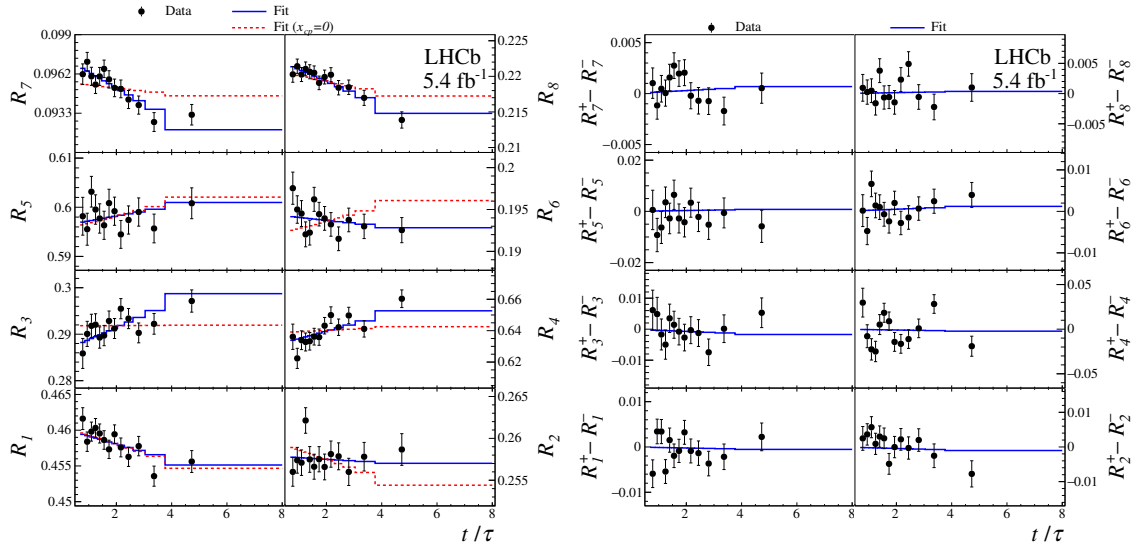


**Figure 10.** (Left)  $CP$ -averaged yield ratios and (right) ratio differences of  $D^0$  and  $\bar{D}^0$  decays into the  $K_S^0\pi^+\pi^-$  final state as a function of decay time, for each Dalitz-plot bin. Any deviations from constant functions would indicate the presence of (left) mixing or (right)  $CP$  violation. Fit projections are overlaid. The dashed red line in the left plot corresponds to the projection of a fit where the parameter  $x_{CP}$  is fixed to zero. Figures taken from ref. [151].

the sample collected in *Run 1* [153], thanks to improved triggering [65]. The selection requirements introduce correlations between the decay time and the Dalitz coordinates, in particular  $m^2(\pi^+\pi^-)$ . Regions of constant  $m^2(\pi^+\pi^-)$  correspond to bands orthogonal to the bisector; see for example the  $\rho(770)^0$  lineshape in fig. 9 right. Therefore, a decorrelation procedure is applied by weighting the time distribution of the sum of the candidates in pairs of rectangles symmetric with respect to the bisector (see fig. 9 right) to the time distribution of the total sample. Since a nonzero value of  $x_{CP}$  has the effect of moving candidates into the position symmetric with respect to the bisector, the procedure does not bias this variable, whereas second-order biases to  $y_{CP}$  are corrected for. Momentum-dependent detection asymmetries of the  $\pi^+$  and  $\pi^-$  mesons also do not cancel in the ratios. They are corrected for based on a measurement of kinematically weighted  $D_s^+ \rightarrow \pi^+\pi^-\pi^+$  CF decays, where the additional  $D_s^+$  production asymmetry and the detection asymmetry of the third pion are removed by subtraction with  $D_s^+ \rightarrow \phi(1020)\pi^+$  CF decays followed by  $\phi(1020) \rightarrow K^+K^-$ . This takes advantage of the fact that the detection asymmetry of the kaon pair is zero, as the  $\phi(1020)$  decay is self-conjugate and its decay width is small, while the same is not true for the resonant structure of the pion pair of  $D_s^+ \rightarrow \pi^+\pi^-\pi^+$  decays.

The projections of the fits to the corrected time-dependent ratios are shown in fig. 10. The results for the mixing and  $CP$  violation parameters are, after averaging with a more recent but threefold less precise measurement based on the *Run 2*  $\mu^-$ -tagged sample [154],

$$\begin{aligned} x_{CP} &= (4.00 \pm 0.45 \pm 0.20) \times 10^{-3}, & \Delta x &= (-0.29 \pm 0.18 \pm 0.01) \times 10^{-3}, \\ y_{CP} &= (5.51 \pm 1.16 \pm 0.59) \times 10^{-3}, & \Delta y &= (0.31 \pm 0.35 \pm 0.13) \times 10^{-3}, \end{aligned}$$

where the statistical uncertainties include a component from the external knowledge of the

strong-phase differences [150, 152], which accounts for approximately 50% of the uncertainties of  $x_{CP}$  and  $y_{CP}$ . The systematic uncertainties on  $x_{CP}$  and  $y_{CP}$  are mainly due to neglecting the finite resolution of the Dalitz variables, to the assumption that the selection efficiency is constant across each Dalitz bin, and to the decorrelation procedure between decay time and the Dalitz coordinates. The parameters  $\Delta x$  and  $\Delta y$  are compatible with zero within 1.4 standard deviations, in agreement with the hypothesis of no  $CP$  violation. The determinations of  $x_{CP}$  and  $\Delta x$  improve the precision of their world average by a factor of 3, and the former constitutes the first observation of a nonzero mass difference between the neutral charmed-meson mass eigenstates, with a significance greater than 7 standard deviations. Furthermore, it confirms that the phase  $\phi_2^M$  is approximately equal to zero rather than  $\pi$ , implying that the shorter-lived and nearly  $CP$ -even eigenstate is also heavier.

### 5.3 Measurement of the decay-width difference of the neutral charmed-mesons mass eigenstates with $D^0 \rightarrow K^+K^-$ and $D^0 \rightarrow \pi^+\pi^-$ decays

The  $y_{CP}$  parameter introduced in eq. (5.3), given the current constraints on the size of  $\phi_2^\Gamma$  [146], is nearly indistinguishable from the mixing parameter  $y_{12}$ , and provides the cleanest access to this observable. It can be also measured with other decay channels [155–159]; currently, the best precision is achieved using  $D^0 \rightarrow K^+K^-$  and  $D^0 \rightarrow \pi^+\pi^-$  decays. Due to mixing, the time distribution of  $D^0$  decays into these  $CP$  eigenstates differs from an exponential and receives first-order corrections proportional to  $y_{CP}$ . To measure this tiny deviation, it is essential to calibrate the measurement on a reference channel. This would ideally be a flavour-specific decay such as a leptonic decay,  $D^0 \rightarrow K^-\ell^+\nu_\ell$ . Owing to the poor mass resolution due to the missing neutrino, and to the desire to keep the selection as close as possible to that of the signal channel,  $D^0 \rightarrow K^-\pi^+$  decays are usually preferred. Here the contribution of mixing is not negligible; however, it is suppressed with respect to the decays into the  $CP$  eigenstates, since the decay amplitude following mixing is DCS rather than CF (whereas for the  $CP$  eigenstates both the decay amplitudes without and following mixing are CS). The time-dependent ratio of the decay rates of the signal and calibration channels is equal to [72]

$$\frac{\Gamma(D^0 \rightarrow f, t) + \Gamma(\bar{D}^0 \rightarrow f, t)}{\Gamma(D^0 \rightarrow K^-\pi^+, t) + \Gamma(\bar{D}^0 \rightarrow K^+\pi^-, t)} \approx \text{const.} \times \left\{ 1 - (y_{CP} - y_{CP}^{K^-\pi^+}) \frac{t}{\tau_{D^0}} + \left[ \frac{1}{4}(x_{12}^2 + y_{12}^2) + y_{CP}^{K^-\pi^+} (y_{CP}^{K^-\pi^+} - y_{CP}) \right] \left( \frac{t}{\tau_{D^0}} \right)^2 \right\}, \quad (5.4)$$

where  $f$  stands for  $K^+K^-$  or  $\pi^+\pi^-$ , the size of  $y_{CP}^{K^-\pi^+}$  is around 6% of that of  $y_{CP}$  (this value is approximately equal to the ratio of the magnitudes of the DCS to CF decay amplitudes) and its sign is the opposite of that of  $y_{CP}$ , and the selection efficiencies cancel to a large extent in the ratio.<sup>10</sup>

<sup>10</sup>The observable  $y_{CP}$  in eq. (5.4) should actually be  $y_{CP}^f$ , defined analogously to  $y_{CP}$  in eq. (5.3), but with the substitution  $\phi_2^\Gamma \rightarrow \phi_f^\Gamma \equiv \arg(\bar{A}_f \Gamma_{12} / A_f)$ . Since  $\phi_f^\Gamma / \phi_2^\Gamma = 1 + \mathcal{O}(\epsilon)$ , where the parameter  $\epsilon \approx 0.3$  quantifies  $U$ -spin breaking [21], and the dependence of  $y_{CP}^f$  on  $\phi_f^\Gamma$  is at second order, this difference is negligible.

This ratio has been recently measured by the LHCb collaboration employing the  $D^{*+}$ -tagged data sample collected in *Run 2* [148, 160]. The measurement requires the time-dependent ratio of the selection efficiencies at numerator and denominator to be controlled with a precision better than the absolute uncertainty on  $y_{CP}$ , that is close to  $10^{-4}$  level. This is achieved by employing trigger lines designed to minimise the variation of the efficiency as a function of decay time, in particular by avoiding requirements on displacement-related variables [161]. The main differences between the selection efficiencies of the signal and calibration channels are a consequence of the different masses of the final-state particles, which result in different momenta and opening angles of the two hadrons at equal  $D^0$  momentum. This effect is corrected for as follows: for each  $D^0 \rightarrow K^+K^-$  decay, the momentum and direction of each kaon are recomputed under the hypothesis that the mass of the positively charged kaon be equal to that of a pion, keeping constant the decay angle in the  $D^0$  rest frame. The kinematics of the  $D^0 \rightarrow K^+K^-$  decay is thus transformed into the one that it would have had if its final state had been  $K^-\pi^+$ . After this “kinematic matching”, the same requirements on the momentum and IP of the particles are applied to both the  $D^0 \rightarrow K^-\pi^+$  decay and the transformed  $D^0 \rightarrow K^+K^-$  decay. The requirements are tighter than the trigger requirements across the whole available phase-space, to ensure equal selection efficiencies for the two decay channels. An analogous procedure is employed to transform the  $D^0 \rightarrow K^-\pi^+$  kinematics into that of  $D^0 \rightarrow \pi^+\pi^-$  decays. Second order differences due to different particle identification efficiencies and to detection asymmetries that are momentum-dependent are removed by equalising the momentum distributions of the signal and calibration samples, assigning per-candidate weights. The method is validated in simulation and by applying it also to the time-dependent ratio of  $D^0 \rightarrow K^+K^-$  to  $D^0 \rightarrow \pi^+\pi^-$  decays, for which the relative kinematic differences are larger. This ratio is verified to be compatible with a constant, as expected, within an uncertainty of  $0.5 \times 10^{-3}$ . Finally, the contribution of secondary mesons is explicitly accounted for, with a procedure similar to that described in section 5.1.

The exponential fits to the yields ratios of the signal and calibration channels after the corrections above are shown in fig. 11. The results of the two measurements are in agreement with each other. Neglecting final-state dependent effects, their average is

$$y_{CP} - y_{CP}^{K^-\pi^+} = (6.96 \pm 0.26 \pm 0.13) \times 10^{-3},$$

where the largest systematic uncertainties are due to the subtraction of the combinatorial background from random  $D^0\text{-}\pi^+$  associations, and to the background of misreconstructed multibody  $D^0$  decays. This result is more precise than the previous world average [146, 156–158] by a factor of four, and improves significantly our knowledge of  $y_{12}$ , as shown in the next sections.

#### 5.4 Improvement in the knowledge of the mixing parameters

The improvement in the knowledge of the parameters of charm mixing and of  $CP$  violation in the mixing following the measurements described in the previous sections is shown in fig. 12. The new world averages are

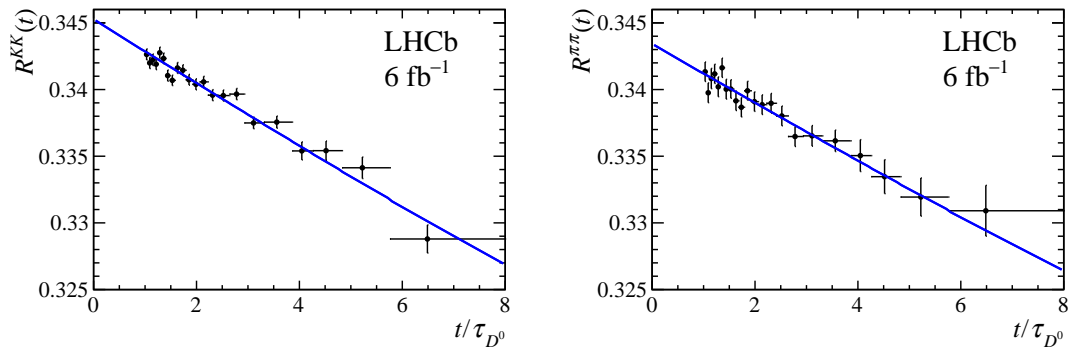


**Figure 11.** Ratio of the yields of (left)  $D^0 \rightarrow K^+K^-$  and (right)  $D^0 \rightarrow \pi^+\pi^-$  decays to that of  $D^0 \rightarrow K^-\pi^+$  decays, after the kinematic matching and equalisation. An exponential fit is superimposed, where the deviation from a constant indicates the presence of nonzero  $y_{CP} - y_{CP}^{K^-\pi^+}$ . Differences between the quadratic term of eq. (5.4) and that of the Taylor series of the exponential are accounted for among the systematic uncertainties. Figure taken from ref. [148].

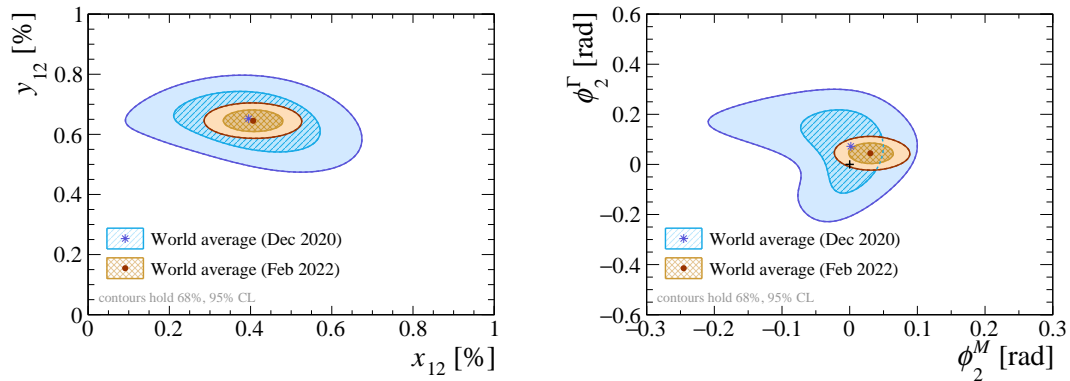


**Figure 12.** Improvement in the knowledge of the parameters of (left) mixing and (right)  $CP$ -violation in the mixing of  $D^0$  mesons, following the measurements presented in sections 5.1 to 5.3. The black cross in the right plot corresponds to the case of no  $CP$  violation. The improvements in  $x_{12}$  and  $\phi_2^\Gamma$  are driven by the measurement of  $D^0 \rightarrow K_S^0 \pi^+ \pi^-$  decays, while the improvement in  $y_{12}$  is driven by the measurement of  $y_{CP}$ . The precision on  $\phi_2^M$  improves thanks to the interplay of the new measurement of  $\Delta Y$  and to the improved precision on  $x_{12}$  and  $y_{12}$ , which enhances the sensitivity to  $\phi_2^M$  from measurements of both  $\Delta Y$  and  $D^0 \rightarrow K^+ \pi^-$  decays [147]. Both plots have been produced using the public code in ref. [22].

$$\begin{aligned}
 x_{12} &= (4.06 \pm 0.44) \times 10^{-3}, & \phi_2^M &= (0.031 \pm 0.021) \text{ rad}, \\
 y_{12} &= (6.47 \pm 0.24) \times 10^{-3}, & \phi_2^\Gamma &= (0.047 \pm 0.027) \text{ rad},
 \end{aligned}$$

and improve by more than a factor of two with respect to the previous determinations. The precision on the  $CP$ -violation mixing phases is still around one order of magnitude larger than the SM predictions, and their best-point estimates agree with the hypothesis of no  $CP$  violation within slightly less than two standard deviations. Further investigations with additional decay channels and with the data from the upcoming LHCb upgrade are

needed to clarify whether this is a statistical fluctuation or not.

### 5.5 First simultaneous combination of charm and beauty measurements

The precision on the mixing parameters can be further improved by combining charm measurements with those of the angle  $\gamma$  of the CKM unitarity triangle [31, 162, 163]. The most precise measurements of  $\gamma$  to date employ  $B^+ \rightarrow DK^+$  and  $B^+ \rightarrow D\pi^+$  decays, where  $D$  stands for either of  $D^0$  or  $\bar{D}^0$  mesons reconstructed in a final state that is shared by the two mesons. The final states  $K_S^0\pi^+\pi^-$  and  $K^-\pi^+$  are the most relevant [163, 164]; see fig. 13 left. In particular, the rate of the decays where the  $D$  meson is reconstructed in the  $K^-\pi^+$  final states is equal to

$$\begin{aligned} \Gamma(B^\pm \rightarrow (K^\mp\pi^\pm)_D h^\pm) &\propto |r_D^{K\pi} e^{-i\delta_D^{K\pi}} + r_B^{Dh} e^{i(\delta_B^{Dh} \pm \gamma)}|^2 \\ &= (r_D^{K\pi})^2 + (r_B^{Dh})^2 + r_D^{K\pi} r_B^{Dh} \cos(\delta_D^{K\pi} + \delta_B^{Dh} \pm \gamma), \end{aligned} \quad (5.5)$$

where  $r_B^{Dh} e^{i(\delta_B^{Dh} + \gamma)}$  is the ratio of the  $B^+ \rightarrow D^0 h^+$  to  $B^+ \rightarrow \bar{D}^0 h^+$  decay amplitudes,  $r_D^{K\pi} e^{-i\delta_D^{K\pi}}$  is the ratio between the  $\bar{D}^0 \rightarrow K^-\pi^+$  and  $D^0 \rightarrow K^-\pi^+$  decay amplitudes, and subleading effects from charm mixing [162] are neglected for the sake of simplicity.<sup>11</sup> However, the measurement of these decay rates does not allow for an unambiguous determination of  $\gamma$  nor of the strong phases, since the cosine function in eq. (5.5) is not injective [165]; see fig. 13 left. By contrast, multibody  $D^0$  decay channels such as  $D \rightarrow K_S^0\pi^+\pi^-$  allow, in combination with external inputs for the charm hadronic parameters [150, 152], for an unambiguous measurement of  $\gamma$ . In fact, the variation of the strong phase,  $\delta_D^{K_S^0\pi^+\pi^-}$ , as a function of the phase space allows the trigonometric degeneracy to be resolved; then not only  $\gamma$ , but also  $r_B^{Dh}$  and  $\delta_B^{Dh}$ , which are independent of the  $D$  final state, can be measured [166].

The combination of the measurements of the  $K^-\pi^+$  and  $K_S^0\pi^+\pi^-$  final states improves the precision not only for  $\gamma$  and  $\delta_B^{Dh}$  (see fig. 13 left) but, through eq. (5.5), also for  $\delta_D^{K\pi}$ . This has a beneficial effect on the knowledge of charm mixing parameters, since one of the most precise measurements of mixing is that of the observable  $y' \equiv -y_{12} \cos \delta_D^{K\pi} + x_{12} \sin \delta_D^{K\pi}$  in  $D^0 \rightarrow K^+\pi^-$  decays [147], and the uncertainty on  $\delta_D^{K\pi}$  has limited the precision of its interpretation in terms of the mixing parameters for a long time.

A new simultaneous combination of  $\gamma$  and charm measurements has recently been performed that allows the precision on  $\delta_D^{K\pi}$  to be improved by a factor of two [31]. Since the  $U$ -spin breaking difference of  $\delta_D^{K\pi}$  from  $\pi$  is small,  $y'$  is mostly sensitive to  $y_{12}$ . Therefore, the precision on  $y_{12}$  is also improved by around a factor of 2. This improvement is comparable to that allowed by the  $y_{CP}$  measurement that was published shortly after the combination, and the two results show excellent agreement; see fig. 13 right.

The benefits of a simultaneous combination could be even larger in future studies of multibody decays such as  $D^0 \rightarrow K^\pm\pi^\mp\pi^+\pi^-$ , whose contribution to the determination of both the  $\gamma$  angle and charm mixing and  $CP$  violation is limited by the knowledge of the relevant  $D^0$  hadronic parameters (strong-phase differences and amplitude ratios) as a

<sup>11</sup>Note that a rigorous definition of the strong phases should be based on the full  $B^+ \rightarrow D(\rightarrow f)h^+$  decay chain, as the individual ratios of amplitudes are not quark- nor meson-rephasing invariant.

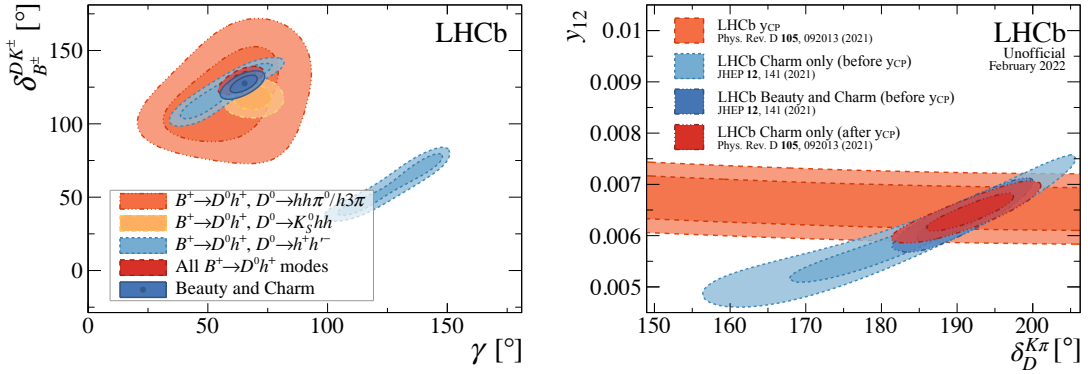


**Figure 13.** (Left) Two-dimensional confidence regions for the CKM angle  $\gamma$  and for the strong-phase difference  $\delta_B^{DK}$ , for different  $D$  decay channels and for their combination. (Right) Two-dimensional confidence region for the mixing parameter  $y_{12}$  and for the strong-phase difference  $\delta_D^{K\pi}$ . The correlation in the blue and red contours is due to the measurement of  $y'$  in  $D^0 \rightarrow K^+\pi^-$  decays [147]. Both the simultaneous combination of  $\gamma$  and charm measurements, and the inclusion of the  $y_{CP}$  measurement discussed in section 5.3, improve the precision on  $y_{12}$  and on  $\delta_D^{K\pi}$  by around a factor of two. Figures taken from refs. [31, 148].

function of phase space [167]. The combination would indirectly improve the knowledge of these parameters, thanks to the different way in which they enter the mixing and  $CP$  violation observables measured in the  $B^+ \rightarrow Dh^\pm$  and  $D^0$  decays into the same phase-space regions. In this case, the combination may improve the precision not only for the charm sector, but also for the angle  $\gamma$  [167–169].

## 6 Conclusions and prospects

The study of charm mixing and  $CP$  violation constitutes a unique tool to test the up-type quark sector of CKM paradigm. After many years of frustrated experimental searches, this field is eventually entering the era of precision studies. This implies new challenges in the theoretical interpretation of the results, whose precision is limited by the understanding of strong interactions at the energy scale of the charm mass. In particular, the compatibility of the historic first observation of  $CP$  violation in  $D^0 \rightarrow K^+K^-$  and  $D^0 \rightarrow \pi^+\pi^-$  decays with the SM constitutes an open puzzle. A parallel progress of the theoretical tools and of the experimental studies of  $CP$  violation and rescattering is needed to shed light on this issue. This review presented the most recent measurements of mixing and  $CP$  violation performed with the data collected at the LHCb experiment — the major player of this experimental endeavour — during its *Run 2* (2015–2018).

Apart from the non-zero value of  $\Delta A_{CP}$ , all other searches for  $CP$  violation have so far yielded null results. However, a very recent measurement of  $A_{CP}(D^0 \rightarrow K^+K^-)$  indirectly establishes the first evidence for of  $CP$  violation in a single decay channel,  $D^0 \rightarrow \pi^+\pi^-$ . In addition, significant improvements in precision are obtained in decay channels with neutral particles such as  $D^0 \rightarrow K_S^0 K_S^0$  and  $D_{(s)}^+ \rightarrow h^0 h^+$ . Many of these measurements achieve world-leading precisions, at the per cent level or below, despite the challenges posed by



their study at hadron colliders. The potential of the *Run 2* dataset is not exhausted yet, and many new measurements are expected in the next few years, especially for multibody decays.

Even larger improvements in precision have been obtained in time-dependent measurements, which determined the value of the mixing parameters  $x_{12}$  and  $y_{12}$  with 12% and 4% relative uncertainty, respectively. The weak phases responsible for  $CP$  violation in the mixing are still compatible with zero (though in slight tension at the level of around two standard deviations), within uncertainties of around 25 mrad. This value is one order of magnitude larger than the SM estimates. The prospect of using multibody decays such as  $D^0 \rightarrow K^\pm \pi^\mp \pi^+ \pi^-$  to improve the precision on these phases and on the mixing parameters looks particularly attractive. The improvement of the trigger between *Run 1* and *Run 2* significantly increased the yield per integrated luminosity of multibody decays; see for example ref. [151]. Moreover, while their analysis is complicated by the five-dimensional phase space of the final state, the interplay with the measurements of  $B \rightarrow (K^\pm \pi^\mp \pi^+ \pi^-)_{Dh^+}$  decays might indirectly improve the precision also on the angle  $\gamma$  of the CKM unitarity triangle [168, 169].

In the end, it is likely that larger data samples will be needed to yield the first observation of  $CP$  violation in a single decay channel and of  $CP$  violation in the mixing. All current measurements are statistically limited, and no irreducible systematic uncertainties have been pinpointed yet. Therefore, several experiments are planned to improve the statistical precision of these measurements by increasing the size of the collected samples. In the near future, the Belle II experiment is expected to contribute significantly to the studies of final states with neutral particles [170], whereas the upcoming LHCb Upgrade I will yield the best precision for all other final states. The latter plans to increase the collected integrated luminosity to  $25 \text{ fb}^{-1}$  ( $50 \text{ fb}^{-1}$ ) by the end of *Run 3* (*Run 4*), scheduled to take place from 2022 to 2025 (from 2029 to 2032). This will be obtained by increasing the instantaneous luminosity fivefold, reaching a value of  $2 \times 10^{33} \text{ cm}^{-2} \text{ s}^{-1}$ , and the centre-of-mass energy to 14 TeV [59, 60]. Another crucial improvement of this upgrade will be the removal of the hardware trigger, whose thresholds were often tighter than those affordable in the software trigger and in the offline analysis of charm decays. The possibility to reconstruct all collision events in the software will not only improve the collection efficiency, but also reduce the detection asymmetry due to triggering with the hadronic calorimeter. In addition, the greater flexibility in the design of the trigger selections will be beneficial in reducing the correlations between decay time and kinematics introduced by the trigger requirements, and to keep systematic uncertainties such as those described in sections 5.1 and 5.2 at a low level. Finally, the introduction of new trigger lines dedicated to displaced  $K_S^0$  mesons in the first level of the software trigger will significantly benefit the collection efficiency of decays including these particles in their final state. To take full advantage of the increased collected yields also in the study of multibody decays, improving the knowledge of the charm hadronic parameters of decays such as  $D^0 \rightarrow K_S^0 \pi^+ \pi^-$  and  $D^0 \rightarrow K^\pm \pi^\mp \pi^+ \pi^-$  will be essential. The existing BESIII charm factory should therefore be upgraded, or new ones should be built [171–173].

In the long term, an Upgrade II of the LHCb experiment has been proposed to in-

crease the integrated luminosity to about  $300 \text{ fb}^{-1}$  [174, 175]. While the experimental and computational challenges of operating a detector at an instantaneous luminosity larger by a factor of ten than that of the Upgrade I,  $2 \times 10^{34} \text{ cm}^{-2} \text{ s}^{-1}$ , are formidable, this would be a unique opportunity to reduce the current statistical uncertainties by nearly one order of magnitude. This might allow to eventually detect  $CP$  violation in  $D^0$  mixing, as well as to measure the  $CP$  asymmetries of a variety of decay channels with precision ranging from below  $10^{-4}$  to  $10^{-3}$ . Sixty years after the November revolution [176–178], a complete picture of the phenomenology of charm-quark decays may thus eventually be achieved.

## Acknowledgments

I am grateful to the editors of Modern Physics Letters A for inviting me to write this review, and to the participants to the 2022 MIAPP workshop “Charming clues for existence” for stimulating discussions. I am especially indebted to Alex Gilman and to Guy Wilkinson for proofreading the manuscript and for providing valuable comments. I thank Adam Davis for pointing out some typos in eq. (2.2) and its analogue for  $M_{1,0}$  in the manuscript. This work has been supported in part by the Science and Technology Facilities Council [grant number ST/S000933/1], and has benefitted from the support of the Munich Institute for Astro- and Particle Physics (MIAPP), which is funded by the Deutsche Forschungsgemeinschaft (DFG, German Research Foundation) under Germany Excellence Strategy [EXC-2094/390783311].

## References

- [1] S. Glashow, J. Iliopoulos and L. Maiani, *Weak interactions with lepton-hadron symmetry*, *Phys. Rev. D* **2** (1970) 1285.
- [2] A. Buras, *Gauge theories of weak decays*, pp. 71–73, Cambridge University Press (2020), DOI.
- [3] R.D. Peccei, *The strong CP problem and axions*, *Lect. Notes Phys.* **741** (2008) 3 [hep-ph/0607268].
- [4] N. Cabibbo, *Unitary symmetry and leptonic decays*, *Phys. Rev. Lett.* **10** (1963) 531.
- [5] M. Kobayashi and T. Maskawa, *CP-violation in the renormalizable theory of weak interaction*, *Prog. Theor. Phys.* **49** (1973) 652.
- [6] PARTICLE DATA GROUP, *Review of particle physics*, *Prog. Theor. Exp. Phys.* **2020** (2020) 083C01, see review therein.
- [7] M. Bott-Bodenhausen et al., *Search for decay of neutral kaons into charged lepton pairs*, *Phys. Lett. B* **24** (1967) 194 [Erratum *ibid* **24** (1967) 352].
- [8] H. Foeth et al., *Search for  $K_L \rightarrow \mu^+ \mu^-$  and  $K_L \rightarrow e^+ e^-$  decays*, *Phys. Lett. B* **30** (1969) 282.
- [9] J. Christenson, J. Cronin, V. Fitch and R. Turlay, *Evidence for the  $2\pi$  decay of the  $K_2^0$  meson*, *Phys. Rev. Lett.* **13** (1964) 138.
- [10] B.A. Campbell and P.J. O’Donnell, *Mass of the top quark and induced decay and mixing of neutral B mesons*, *Phys. Rev. D* **25** (1982) 1989.
- [11] ARGUS collaboration, *Observation of  $B^0-\bar{B}^0$  mixing*, *Phys. Lett. B* **192** (1987) 245.

- [12] M. Dine and A. Kusenko, *The origin of the matter–antimatter asymmetry*, *Rev. Mod. Phys.* **76** (2003) 1 [[hep-ph/0303065](#)].
- [13] CKMFITTER GROUP, *CP violation and the CKM matrix: Assessing the impact of the asymmetric B factories*, *Eur. Phys. J. C* **41** (2005) 1 [[hep-ph/0406184](#)], updated results and plots available at <http://ckmfitter.in2p3.fr/>.
- [14] Y. Grossman, A.L. Kagan and Y. Nir, *New physics and CP violation in singly Cabibbo suppressed D decays*, *Phys. Rev. D* **75** (2007) 036008 [[hep-ph/0609178](#)].
- [15] F. Buccella, M. Lusignoli, G. Miele, A. Pugliese and P. Santorelli, *Nonleptonic weak decays of charmed mesons*, *Phys. Rev. D* **51** (1995) 3478 [[hep-ph/9411286](#)].
- [16] H. Gisbert, M. Golz and D.S. Mitzel, *Theoretical and experimental status of rare charm decays*, *Mod. Phys. Lett. A* **36** (2021) 2130002 [[arXiv:2011.09478](#)].
- [17] LHCb collaboration, *Angular analysis of  $D^0 \rightarrow \pi^+\pi^-\mu^+\mu^-$  and  $D^0 \rightarrow K^+K^-\mu^+\mu^-$  decays and search for CP violation*, *Phys. Rev. Lett.* **128** (2022) 221801 [[arXiv:2111.03327](#)].
- [18] LHCb collaboration, *Search for rared decays of  $D^0$  mesons into two muons*, in preparation, to be submitted to *Phys. Rev. Lett.* Online at <https://agenda.infn.it/event/28874/contributions/169350/>.
- [19] Y. Grossman, Y. Nir and G. Perez, *Testing new indirect CP violation*, *Phys. Rev. Lett.* **103** (2009) 071602 [[arXiv:0904.0305](#)].
- [20] A.L. Kagan and M.D. Sokoloff, *Indirect CP violation and implications for  $D^0-\bar{D}^0$  and  $B_s^0-\bar{B}_s^0$  mixing*, *Phys. Rev. D* **80** (2009) 076008 [[arXiv:0907.3917](#)].
- [21] A.L. Kagan and L. Silvestrini, *Dispersive and absorptive CP violation in  $D^0-\bar{D}^0$  mixing*, *Phys. Rev. D* **103** (2021) 053008 [[arXiv:2001.07207](#)].
- [22] T. Pajero, *Fitter of charm mixing and CP violation parameters*, October 2021, online at <https://github.com/tpajero/charm-fitter>.
- [23] M. Chala, A. Lenz, A.V. Rusov and J. Scholtz,  *$\Delta A_{CP}$  within the Standard Model and beyond*, *JHEP* **07** (2019) 161 [[arXiv:1903.10490](#)].
- [24] A.F. Falk, Y. Grossman, Z. Ligeti and A.A. Petrov,  *$SU(3)$  breaking and  $D^0-\bar{D}^0$  mixing*, *Phys. Rev. D* **65** (2002) 054034 [[hep-ph/0110317](#)].
- [25] M. Gronau and J.L. Rosner, *Revisiting  $D^0-\bar{D}^0$  mixing using U-spin*, *Phys. Rev. D* **86** (2012) 114029 [[arXiv:1209.1348](#)].
- [26] D. King, A. Lenz, M.L. Piscopo, T. Rauh, A.V. Rusov and C. Vlahos, *Revisiting inclusive decay widths of charmed mesons*, *JHEP* **08** (2022) 241 [[arXiv:2109.13219](#)].
- [27] A. Lenz and G. Wilkinson, *Mixing and CP violation in the charm system*, *Annual Review of Nuclear and Particle Science* **71** (2021) 1 [[arXiv:2011.04443](#)].
- [28] M.T. Hansen and S.R. Sharpe, *Multiple-channel generalization of Lellouch–Lüscher formula*, *Phys. Rev. D* **86** (2012) 016007 [[arXiv:1204.0826](#)].
- [29] H.-Y. Cheng and C.-W. Chiang, *Long-distance contributions to  $D^0-\bar{D}^0$  mixing parameters*, *Phys. Rev. D* **81** (2010) 114020 [[arXiv:1005.1106](#)].
- [30] H.-Y. Jiang, F.-S. Yu, Q. Qin, H.-n. Li and C.-D. Lü,  *$D^0-\bar{D}^0$  mixing parameter  $y$  in the factorization-assisted topological-amplitude approach*, *Chin. Phys. C* **42** (2018) 063101 [[arXiv:1705.07335](#)].
- [31] LHCb collaboration, *Simultaneous determination of CKM angle  $\gamma$  and charm mixing parameters*, *JHEP* **12** (2021) 141 [[arXiv:2110.02350](#)].
- [32] A.F. Falk, Y. Grossman, Z. Ligeti, Y. Nir and A.A. Petrov,  *$D^0-\bar{D}^0$  mass difference from a dispersion relation*, *Phys. Rev. D* **69** (2004) 114021 [[hep-ph/0402204](#)].

- [33] I.I. Bigi, A. Paul and S. Recksiegel, *Conclusions from CDF results on CP Violation in  $D^0 \rightarrow \pi^+\pi^-, K^+K^-$  and future tasks*, *JHEP* **06** (2011) 089 [[arXiv:1103.5785](#)].
- [34] M. Bobrowski, A. Lenz, J. Riedl and J. Rohrwild, *How large can the SM contribution to CP violation in  $D^0 - \bar{D}^0$  mixing be?*, *JHEP* **03** (2010) 009 [[arXiv:1002.4794](#)].
- [35] H.-N. Li, H. Umeeda, F. Xu and F.-S. Yu, *D meson mixing as an inverse problem*, *Phys. Lett. B* **810** (2020) 135802 [[arXiv:2001.04079](#)].
- [36] E. Golowich, J. Hewett, S. Pakvasa and A.A. Petrov, *Implications of  $D^0 - \bar{D}^0$  mixing for new physics*, *Phys. Rev. D* **76** (2007) 095009 [[arXiv:0705.3650](#)].
- [37] N. Carrasco et al.,  *$D^0 - \bar{D}^0$  mixing in the standard model and beyond from  $N_f = 2$  twisted mass QCD*, *Phys. Rev. D* **90** (2014) 014502 [[arXiv:1403.7302](#)].
- [38] ETM collaboration,  *$\Delta S=2$  and  $\Delta C=2$  bag parameters in the standard model and beyond from  $N_f = 2 + 1 + 1$  twisted-mass lattice QCD*, *Phys. Rev. D* **92** (2015) 034516 [[arXiv:1505.06639](#)].
- [39] A. Bazavov et al., *Short-distance matrix elements for  $D^0$ -meson mixing for  $N_f = 2 + 1$  lattice QCD*, *Phys. Rev. D* **97** (2018) 034513 [[arXiv:1706.04622](#)].
- [40] M. Kirk, A. Lenz and T. Rauh, *Dimension-six matrix elements for meson mixing and lifetimes from sum rules*, *JHEP* **12** (2017) 068 [Erratum *ibid* **06** (2020) 162] [[arXiv:1711.02100](#)].
- [41] C. Alpigiani et al., *Unitarity triangle analysis in the Standard Model and beyond*, [[arXiv:1710.09644](#)].
- [42] S. Bergmann and Y. Nir, *New physics effects in doubly Cabibbo suppressed D decays*, *JHEP* **09** (1999) 031 [[hep-ph/9909391](#)].
- [43] I.I.Y. Bigi and H. Yamamoto, *Interference between Cabibbo allowed and doubly forbidden transitions in  $D \rightarrow K_{S,L} + \pi$ 's decays*, *Phys. Lett. B* **349** (1995) 363 [[hep-ph/9502238](#)].
- [44] J. Brod, Y. Grossman, A.L. Kagan and J. Zupan, *A consistent picture for large penguins in  $D \rightarrow \pi^+\pi^-, K^+K^-$* , *JHEP* **10** (2012) 161 [[arXiv:1203.6659](#)].
- [45] S. Müller, U. Nierste and S. Schacht, *Topological amplitudes in D decays to two pseudoscalars: A global analysis with linear  $SU(3)_F$  breaking*, *Phys. Rev. D* **92** (2015) 014004 [[arXiv:1503.06759](#)].
- [46] E. Franco, S. Mishima and L. Silvestrini, *The Standard Model confronts CP violation in  $D^0 \rightarrow \pi^+\pi^-$  and  $D^0 \rightarrow K^+K^-$* , *JHEP* **05** (2012) 140 [[arXiv:1203.3131](#)].
- [47] J. Brod, A.L. Kagan and J. Zupan, *Size of direct CP violation in singly Cabibbo-suppressed D decays*, *Phys. Rev. D* **86** (2012) 014023 [[arXiv:1111.5000](#)].
- [48] U. Nierste and S. Schacht, *CP Violation in  $D^0 \rightarrow K_S K_S$* , *Phys. Rev. D* **92** (2015) 054036 [[arXiv:1508.00074](#)].
- [49] U. Nierste and S. Schacht, *Neutral  $D \rightarrow KK^*$  decays as discovery channels for charm CP violation*, *Phys. Rev. Lett.* **119** (2017) 251801 [[arXiv:1708.03572](#)].
- [50] S. Schacht and A. Soni, *Enhancement of charm CP violation due to nearby resonances*, *Phys. Lett. B* **825** (2022) 136855 [[arXiv:2110.07619](#)].
- [51] Y. Grossman, A.L. Kagan and J. Zupan, *Testing for new physics in singly Cabibbo suppressed D decays*, *Phys. Rev. D* **85** (2012) 114036 [[arXiv:1204.3557](#)].
- [52] Y. Grossman and D.J. Robinson,  *$SU(3)$  sum rules for charm decay*, *JHEP* **04** (2013) 067 [[arXiv:1211.3361](#)].
- [53] S. Müller, U. Nierste and S. Schacht, *Sum rules of charm CP asymmetries beyond the  $SU(3)_F$  limit*, *Phys. Rev. Lett.* **115** (2015) 251802 [[arXiv:1506.04121](#)].

- [54] LHCb collaboration, *Measurement of B meson production cross-sections in proton-proton collisions at  $\sqrt{s}=7$  TeV*, *JHEP* **08** (2013) 117 [[arXiv:1306.3663](#)].
- [55] LHCb collaboration, *Measurements of prompt charm production cross-sections in pp collisions at  $\sqrt{s}=5$  TeV*, *JHEP* **06** (2017) 147 [[arXiv:1610.02230](#)].
- [56] LHCb collaboration, *The LHCb detector at the LHC*, *JINST* **3** (2008) S08005.
- [57] LHCb collaboration, *LHCb detector performance*, *Int. J. Mod. Phys. A* **30** (2015) 1530022 [[arXiv:1412.6352](#)].
- [58] LHCb collaboration,  *$\bar{b}b$  production angle plots*, online at <https://lhcb.web.cern.ch/lhcb/speakersbureau/html/bb-ProductionAngles.html>.
- [59] LHCb collaboration, *Framework TDR for the LHCb Upgrade: Technical Design Report*, CERN-LHCC-2012-007, 2012.
- [60] LHCb collaboration, *LHCb Trigger and Online Upgrade Technical Design Report*, CERN-LHCC-2014-016, 2014.
- [61] LHCb collaboration, *Prompt charm production in pp collisions at  $\sqrt{s}=7$  TeV*, *Nucl. Phys. B* **871** (2013) 1 [[arXiv:1302.2864](#)].
- [62] LHCb collaboration, *Measurements of prompt charm production cross-sections in pp collisions at  $\sqrt{s}=13$  TeV*, *JHEP* **03** (2016) 159 [Erratum *ibid* **09** (2016) 013] [Erratum *ibid* **05** (2017) 074].
- [63] G. Dujany and B. Storaci, *Real-time alignment and calibration of the LHCb Detector in Run II*, *J. Phys. Conf. Ser.* **664** (2015) 082010.
- [64] R. Aaij et al., *The LHCb trigger and its performance in 2011*, *JINST* **8** (2013) P04022 [[arXiv:1211.3055](#)].
- [65] R. Aaij et al., *Tesla: an application for real-time data analysis in High Energy Physics*, *Comput. Phys. Commun.* **208** (2016) 35 [[arXiv:1604.05596](#)].
- [66] LHCb collaboration, *Search for CP violation in  $D^0 \rightarrow \pi^- \pi^+ \pi^0$  decays with the energy test*, *Phys. Lett. B* **740** (2015) 158 [[arXiv:1410.4170](#)].
- [67] W.E. Johns, *Measurements of the semileptonic decay of the neutral charmed meson  $D^0 \rightarrow K^- \mu^+ \nu_\mu$* , Ph.D. thesis, Colorado U., 1995, FERMILAB-THESIS-1995-05.
- [68] W.D. Hulsbergen, *Decay chain fitting with a Kalman filter*, *Nucl. Instrum. Meth. A* **552** (2005) 566 [[physics/0503191](#)].
- [69] LHCb collaboration, *Observation of CP violation in charm decays*, *Phys. Rev. Lett.* **122** (2019) 211803 [[arXiv:1903.08726](#)].
- [70] F. Betti, *CP violation in  $D^0 \rightarrow K^+ K^-$  and  $D^0 \rightarrow \pi^+ \pi^-$  decays and lepton-flavour universality test with the decay  $B^0 \rightarrow D^{*-} \tau^+ \nu_\tau$* , Ph.D. thesis, Università di Bologna, 2019, CERN-THESIS-2019-016.
- [71] LHCb collaboration, *Search for time-dependent CP violation in  $D^0 \rightarrow K^+ K^-$  and  $D^0 \rightarrow \pi^+ \pi^-$  decays*, *Phys. Rev. D* **104** (2021) 072010 [[arXiv:2105.09889](#)].
- [72] T. Pajero and M.J. Morello, *Mixing and CP violation in  $D^0 \rightarrow K^- \pi^+$  decays*, *JHEP* **03** (2022) 162 [[arXiv:2106.02014](#)].
- [73] LHCb collaboration, *Measurement of indirect CP asymmetries in  $D^0 \rightarrow K^- K^+$  and  $D^0 \rightarrow \pi^- \pi^+$  decays using semileptonic B decays*, *JHEP* **04** (2015) 043 [[arXiv:1501.06777](#)].
- [74] LHCb collaboration, *Measurement of the CP violation parameter  $A_\Gamma$  in  $D^0 \rightarrow K^+ K^-$  and  $D^0 \rightarrow \pi^+ \pi^-$  decays*, *Phys. Rev. Lett.* **118** (2017) 261803 [[arXiv:1702.06490](#)].

- [75] LHCb collaboration, *Updated measurement of decay-time-dependent CP asymmetries in  $D^0 \rightarrow K^+K^-$  and  $D^0 \rightarrow \pi^+\pi^-$  decays*, *Phys. Rev. D* **101** (2020) 012005 [[arXiv:1911.01114](#)].
- [76] LHCb collaboration, *Measurement of CP asymmetry in  $D^0 \rightarrow K^-K^+$  and  $D^0 \rightarrow \pi^-\pi^+$  decays*, *JHEP* **07** (2014) 041 [[arXiv:1405.2797](#)].
- [77] LHCb collaboration, *Measurement of the difference of time-integrated CP asymmetries in  $D^0 \rightarrow K^-K^+$  and  $D^0 \rightarrow \pi^-\pi^+$  decays*, *Phys. Rev. Lett.* **116** (2016) 191601 [[arXiv:1602.03160](#)].
- [78] Y. Grossman and S. Schacht, *The emergence of the  $\Delta U = 0$  rule in charm physics*, *JHEP* **07** (2019) 020 [[arXiv:1903.10952](#)].
- [79] U. Nierste, *Charm decays*, *PoS Beauty2019* (2020) 048 [[arXiv:2002.06686](#)].
- [80] A. Khodjamirian and A.A. Petrov, *Direct CP asymmetry in  $D \rightarrow \pi^-\pi^+$  and  $D \rightarrow K^-K^+$  in QCD-based approach*, *Phys. Lett. B* **774** (2017) 235 [[arXiv:1706.07780](#)].
- [81] A. Dery and Y. Nir, *Implications of the LHCb discovery of CP violation in charm decays*, *JHEP* **12** (2019) 104 [[arXiv:1909.11242](#)].
- [82] R. Bause, H. Gisbert, M. Golz and G. Hiller, *Exploiting CP asymmetries in rare charm decays*, *Phys. Rev. D* **101** (2020) 115006 [[arXiv:2004.01206](#)].
- [83] H.-Y. Cheng and C.-W. Chiang, *Revisiting CP violation in  $D \rightarrow PP$  and  $VP$  decays*, *Phys. Rev. D* **100** (2019) 093002 [[arXiv:1909.03063](#)].
- [84] I. Bediaga, T. Frederico and P. Magalhaes, *Enhanced charm CP asymmetries from final state interactions*, [[arXiv:2203.04056](#)].
- [85] S. Fajfer, P. Singer and J. Zupan, *The Rare decay  $D^0 \rightarrow \gamma\gamma$* , *Phys. Rev. D* **64** (2001) 074008 [[hep-ph/0104236](#)].
- [86] G. Burdman, E. Golowich, J.L. Hewett and S. Pakvasa, *Rare charm decays in the standard model and beyond*, *Phys. Rev. D* **66** (2002) 014009 [[hep-ph/0112235](#)].
- [87] BELLE collaboration, *Search for the rare decay  $D^0 \rightarrow \gamma\gamma$  at Belle*, *Phys. Rev. D* **93** (2016) 051102 [[arXiv:1512.02992](#)].
- [88] H.-n. Li, C.-D. Lu and F.-S. Yu, *Branching ratios and direct CP asymmetries in  $D \rightarrow PP$  decays*, *Phys. Rev. D* **86** (2012) 036012 [[arXiv:1203.3120](#)].
- [89] F. Buccella, A. Paul and P. Santorelli,  *$SU(3)_F$  breaking through final state interactions and CP asymmetries in  $D \rightarrow PP$  decays*, *Phys. Rev. D* **99** (2019) 113001 [[arXiv:1902.05564](#)].
- [90] B. Bhattacharya and J.L. Rosner, *Charmed meson decays to two pseudoscalars*, *Phys. Rev. D* **81** (2010) 014026 [[arXiv:0911.2812](#)].
- [91] D. Pirtskhalava and P. Uttayarat, *CP violation and flavor  $SU(3)$  breaking in  $D$ -meson decays*, *Phys. Lett. B* **712** (2012) 81 [[arXiv:1112.5451](#)].
- [92] H.-Y. Cheng and C.-W. Chiang, *Direct CP violation in two-body hadronic charmed meson decays*, *Phys. Rev. D* **85** (2012) 034036 [Erratum *ibid* **85** (2012) 079903] [[arXiv:1201.0785](#)].
- [93] B. Bhattacharya, M. Gronau and J.L. Rosner, *CP asymmetries in singly-Cabibbo-suppressed  $D$  decays to two pseudoscalar mesons*, *Phys. Rev. D* **85** (2012) 054014 [[arXiv:1201.2351](#)].
- [94] H.-Y. Cheng and C.-W. Chiang,  *$SU(3)$  symmetry breaking and CP violation in  $D \rightarrow PP$  decays*, *Phys. Rev. D* **86** (2012) 014014 [[arXiv:1205.0580](#)].
- [95] G. Hiller, M. Jung and S. Schacht,  *$SU(3)$ -flavor anatomy of nonleptonic charm decays*, *Phys. Rev. D* **87** (2013) 014024 [[arXiv:1211.3734](#)].



- [96] I.I. Bigi, “Could charm ( $\&\tau$ ) transitions be the ‘poor princess’ providing a deeper understanding of fundamental dynamics ?” or: “Finding novel forces”, *Front. Phys. (Beijing)* **10** (2015) 240 [[arXiv:1503.07719](#)].
- [97] X.-G. He and W. Wang, *Flavor SU(3) topological diagram and irreducible representation amplitudes for heavy meson charmless hadronic decays: mismatch and equivalence*, *Chin. Phys. C* **42** (2018) 103108 [[arXiv:1803.04227](#)].
- [98] X.-G. He, Y.-J. Shi and W. Wang, *Unification of flavor SU(3) analyses of heavy hadron weak decays*, *Eur. Phys. J. C* **80** (2020) 359 [[arXiv:1811.03480](#)].
- [99] B. Bhattacharya, A. Datta, A.A. Petrov and J. Waite, *Flavor SU(3) in Cabibbo-favored D-meson decays*, *JHEP* **10** (2021) 024 [[arXiv:2107.13564](#)].
- [100] LHCb collaboration, *Measurement of the time-integrated CP asymmetry in  $D^0 \rightarrow K^+K^-$  decays*, [[arXiv:2209.03179](#)], submitted to *Phys. Rev. Lett.*
- [101] S. Maccolini, *Search for direct CP violation in charm neutral meson decays at LHCb*, Ph.D. thesis, Università di Bologna, 2022, [CERN-THESIS-2022-104](#).
- [102] S. Stahl, *Measurement of CP asymmetry in muon-tagged  $D^0 \rightarrow K^-K^+$  and  $D^0 \rightarrow \pi^-\pi^+$  decays at LHCb*, Ph.D. thesis, University of Heidelberg, 2014, [CERN-THESIS-2014-274](#).
- [103] F.-S. Yu, D. Wang and H.-n. Li, *CP asymmetries in charm decays into neutral kaons*, *Phys. Rev. Lett.* **119** (2017) 181802 [[arXiv:1707.09297](#)].
- [104] LHCb collaboration, *Measurement of CP asymmetry in  $D^0 \rightarrow K^+K^-$  decays*, *Phys. Lett. B* **767** (2017) 177 [[arXiv:1610.09476](#)].
- [105] S. Schacht, *A U-spin anomaly in charm CP violation*, [[arXiv:2207.08539](#)].
- [106] LHCb collaboration, *Measurement of CP asymmetry in  $D^0 \rightarrow K_S^0K_S^0$  decays*, *Phys. Rev. D* **104** (2021) L031102 [[arXiv:2105.01565](#)].
- [107] G. Tuci, *Searching for confirmation of charm CP violation in  $K_S^0$  final states at LHCb*, Ph.D. thesis, Università di Pisa, 2020, [CERN-THESIS-2020-235](#).
- [108] LHCb collaboration, *Measurement of the time-integrated CP asymmetry in  $D^0 \rightarrow K_S^0K_S^0$  decays*, *JHEP* **11** (2018) 048 [[arXiv:1806.01642](#)].
- [109] CLEO collaboration, *Search for CP violation in  $D^0 \rightarrow K_S^0\pi^0$  and  $D^0 \rightarrow \pi^0\pi^0$  and  $D^0 \rightarrow K_S^0K_S^0$  decays*, *Phys. Rev. D* **63** (2001) 071101 [[hep-ex/0012054](#)].
- [110] LHCb collaboration, *Measurement of the time-integrated CP asymmetry in  $D^0 \rightarrow K_S^0K_S^0$  decays*, *JHEP* **10** (2015) 055 [[arXiv:1508.06087](#)].
- [111] BELLE COLLABORATION, *Search for CP violation and measurement of the branching fraction in the decay  $D^0 \rightarrow K_S^0K_S^0$* , *Phys. Rev. Lett.* **119** (2017) 171801 [[arXiv:1705.05966](#)].
- [112] M. Gavrilova, Y. Grossman and S. Schacht, *The mathematical structure of U-spin amplitude sum rules*, *JHEP* **08** (2022) 278 [[arXiv:2205.12975](#)].
- [113] LHCb collaboration, *Search for CP violation in  $D_{(s)}^+ \rightarrow h^+\pi^0$  and  $D_{(s)}^+ \rightarrow h^+\eta$  decays*, *JHEP* **06** (2021) 019 [[arXiv:2103.11058](#)].
- [114] LHCb collaboration, *Measurement of CP asymmetries in  $D_{(s)}^+ \rightarrow \eta\pi^+$  and  $D_{(s)}^+ \rightarrow \eta'\pi^+$  decays*, [[arXiv:2204.12228](#)], submitted to JHEP.
- [115] CLEO collaboration, *Measurements of D meson decays to two pseudoscalar mesons*, *Phys. Rev. D* **81** (2010) 052013 [[arXiv:0906.3198](#)].
- [116] BELLE collaboration, *Observation of  $D^+ \rightarrow K^+\eta^{(\prime)}$  and search for CP violation in  $D^+ \rightarrow \pi^+\eta^{(\prime)}$  decays*, *Phys. Rev. Lett.* **107** (2011) 221801 [[arXiv:1107.0553](#)].



- [117] BELLE collaboration, *Search for CP violation in the  $D^+ \rightarrow \pi^+\pi^0$  decay at Belle*, *Phys. Rev. D* **97** (2018) 011101 [[arXiv:1712.00619](#)].
- [118] BELLE collaboration, *Measurement of branching fractions and CP asymmetries for  $D_s^+ \rightarrow K^+(\eta, \pi^0)$  and  $D_s^+ \rightarrow \pi^+(\eta, \pi^0)$  decays at Belle*, *Phys. Rev. D* **103** (2021) 112005 [[arXiv:2103.09969](#)].
- [119] LHCb collaboration, *Search for CP violation in  $D_s^+ \rightarrow K_S^0\pi^+$ ,  $D^+ \rightarrow K_S^0K^+$  and  $D^+ \rightarrow \phi\pi^+$  decays*, *Phys. Rev. Lett.* **122** (2019) 191803 [[arXiv:1903.01150](#)].
- [120] I. Bediaga, I.I. Bigi, A. Gomes, G. Guerrer, J. Miranda and A.C.d. Reis, *On a CP anisotropy measurement in the Dalitz plot*, *Phys. Rev. D* **80** (2009) 096006 [[arXiv:0905.4233](#)].
- [121] I. Bediaga, J. Miranda, A.C. dos Reis, I.I. Bigi, A. Gomes, J.M. Otalora Goicochea et al., *Second generation of “Miranda procedure” for CP violation in Dalitz studies of B (and D and  $\tau$ ) decays*, *Phys. Rev. D* **86** (2012) 036005 [[arXiv:1205.3036](#)].
- [122] M. Williams, *Observing CP violation in many-body decays*, *Phys. Rev. D* **84** (2011) 054015 [[arXiv:1105.5338](#)].
- [123] M. Gronau and J.L. Rosner, *Triple product asymmetries in K,  $D_{(s)}$  and  $B_{(s)}$  decays*, *Phys. Rev. D* **84** (2011) 096013 [[arXiv:1107.1232](#)].
- [124] G. Durieux and Y. Grossman, *Probing CP violation systematically in differential distributions*, *Phys. Rev. D* **92** (2015) 076013 [[arXiv:1508.03054](#)].
- [125] LHCb collaboration, *Search for CP violation in  $D^+ \rightarrow K^-K^+\pi^+$  decays*, *Phys. Rev. D* **84** (2011) 112008 [[arXiv:1110.3970](#)].
- [126] LHCb collaboration, *Model-independent search for CP violation in  $D^0 \rightarrow K^-K^+\pi^+\pi^-$  and  $D^0 \rightarrow \pi^-\pi^+\pi^-\pi^+$  decays*, *Phys. Lett. B* **726** (2013) 623 [[arXiv:1308.3189](#)].
- [127] LHCb collaboration, *Search for CP violation in the decay  $D^+ \rightarrow \pi^-\pi^+\pi^+$* , *Phys. Lett. B* **728** (2014) 585 [[arXiv:1310.7953](#)].
- [128] LHCb collaboration, *Search for CP violation using T-odd correlations in  $D^0 \rightarrow K^+K^-\pi^+\pi^-$  decays*, *JHEP* **10** (2014) 005 [[arXiv:1408.1299](#)].
- [129] LHCb collaboration, *Search for CP violation in the phase space of  $D^0 \rightarrow \pi^+\pi^-\pi^+\pi^-$  decays*, *Phys. Lett. B* **769** (2017) 345 [[arXiv:1612.03207](#)].
- [130] LHCb collaboration, *Search for CP violation in  $\Xi_c^+ \rightarrow pK^-\pi^+$  decays with model-independent techniques*, *Eur. Phys. J. C* **80** (2020) 986 [[arXiv:2006.03145](#)].
- [131] LHCb collaboration, *Studies of the resonance structure in  $D^0 \rightarrow K_S^0K^\pm\pi^\mp$  decays*, *Phys. Rev. D* **93** (2016) 052018 [[arXiv:1509.06628](#)].
- [132] LHCb collaboration, *Search for CP violation through an amplitude analysis of  $D^0 \rightarrow K^+K^-\pi^+\pi^-$  decays*, *JHEP* **02** (2019) 126 [[arXiv:1811.08304](#)].
- [133] LHCb collaboration, *Studies of the resonance structure in  $D^0 \rightarrow K^\mp\pi^\pm\pi^+\pi^-$  decays*, *Eur. Phys. J. C* **78** (2018) 443 [[arXiv:1712.08609](#)].
- [134] LHCb collaboration, *Amplitude analysis of the  $D^+ \rightarrow \pi^-\pi^+\pi^+$  decay and measurement of the  $\pi^-\pi^+$  S-wave amplitude*, [[arXiv:2208.03300](#)], submitted to *JHEP*.
- [135] LHCb collaboration collaboration, *Amplitude analysis of the  $D_s^+ \rightarrow \pi^-\pi^+\pi^+$  decay*, [[arXiv:2209.09840](#)], submitted to *JHEP*.
- [136] LHCb collaboration collaboration, *Amplitude analysis of the  $\Lambda_c^+ \rightarrow pK^-\pi^+$  decay and  $\Lambda_c^+$  baryon polarization measurement in semileptonic beauty hadron decays*, [[arXiv:2208.03262](#)], submitted to *Phys. Rev. D*.

- [137] F.J. Botella, L.M. Garcia Martin, D. Marangotto, F.M. Vidal, A. Merli, N. Neri et al., *On the search for the electric dipole moment of strange and charm baryons at LHC*, *Eur. Phys. J. C* **77** (2017) 181 [[arXiv:1612.06769](#)].
- [138] A.S. Fomin et al., *Feasibility of measuring the magnetic dipole moments of the charm baryons at the LHC using bent crystals*, *JHEP* **08** (2017) 120 [[arXiv:1705.03382](#)].
- [139] E. Bagli et al., *Electromagnetic dipole moments of charged baryons with bent crystals at the LHC*, *Eur. Phys. J. C* **77** (2017) 828 [Erratum *ibid* **80** (2020) 680] [[arXiv:1708.08483](#)].
- [140] D. Mirarchi, A.S. Fomin, S. Redaelli and W. Scandale, *Layouts for fixed-target experiments and dipole moment measurements of short-lived baryons using bent crystals at the LHC*, *Eur. Phys. J. C* **80** (2020) 929 [[arXiv:1906.08551](#)].
- [141] S. Aiola et al., *Progress towards the first measurement of charm baryon dipole moments*, *Phys. Rev. D* **103** (2021) 072003 [[arXiv:2010.11902](#)].
- [142] T. Pajero, *Search for time-dependent CP violation in  $D^0 \rightarrow K^+K^-$  and  $D^0 \rightarrow \pi^+\pi^-$  decays*, Ph.D. thesis, Scuola Normale Superiore, 2021, [CERN-THESIS-2020-231](#).
- [143] BABAR COLLABORATION, *Measurement of  $D^0-\bar{D}^0$  mixing and CP violation in two-body  $D^0$  decays*, *Phys. Rev. D* **87** (2013) 012004 [[arXiv:1209.3896](#)].
- [144] CDF COLLABORATION, *Measurement of indirect CP-violating asymmetries in  $D^0 \rightarrow K^+K^-$  and  $D^0 \rightarrow \pi^+\pi^-$  decays at CDF*, *Phys. Rev. D* **90** (2014) 111103 [[arXiv:1410.5435](#)].
- [145] BELLE COLLABORATION, *Measurement of  $D^0-\bar{D}^0$  mixing and search for CP violation in  $D^0 \rightarrow K^+K^-$ ,  $\pi^+\pi^-$  decays with the full Belle data set*, *Phys. Lett. B* **753** (2016) 412 [[arXiv:1509.08266](#)].
- [146] HEAVY FLAVOR AVERAGING GROUP, *Averages of b-hadron, c-hadron, and  $\tau$ -lepton properties as of 2018*, *Eur. Phys. J. C* **81** (2021) 226 [[arXiv:1909.12524](#)], updated results and plots available at <https://hflav.web.cern.ch>.
- [147] LHCb collaboration, *Updated determination of  $D^0-\bar{D}^0$  mixing and CP violation parameters with  $D^0 \rightarrow K^+\pi^-$  decays*, *Phys. Rev. D* **97** (2018) 031101 [[arXiv:1712.03220](#)].
- [148] LHCb collaboration, *Measurement of the charm mixing parameter  $y_{CP} - y_{CP}^{K\pi}$  using two-body  $D^0$  meson decays*, *Phys. Rev. D* **105** (2021) 092013 [[arXiv:2202.09106](#)].
- [149] A. Di Canto, J. Garra Tico, T. Gershon, N. Jurik, M. Martinelli, T. Pilař et al., *Novel method for measuring charm-mixing parameters using multibody decays*, *Phys. Rev. D* **99** (2019) 012007 [[arXiv:1811.01032](#)].
- [150] CLEO collaboration, *Model-independent determination of the strong-phase difference between  $D^0$  and  $\bar{D}^0 \rightarrow K_{S,L}^0 h^+ h^-$  ( $h = \pi, K$ ) and its impact on the measurement of the CKM angle  $\gamma/\phi_3$* , *Phys. Rev. D* **82** (2010) 112006 [[arXiv:1010.2817](#)].
- [151] LHCb collaboration, *Observation of the mass difference between neutral charm-meson eigenstates*, *Phys. Rev. Lett.* **127** (2021) 111801 [[arXiv:2106.03744](#)].
- [152] BESIII collaboration, *Model-independent determination of the relative strong-phase difference between  $D^0$  and  $\bar{D}^0 \rightarrow K_{S,L}^0 \pi^+ \pi^-$  and its impact on the measurement of the CKM angle  $\gamma/\phi_3$* , *Phys. Rev. D* **101** (2020) 112002 [[arXiv:2003.00091](#)].
- [153] LHCb collaboration, *Measurement of the mass difference between neutral charm-meson eigenstates*, *Phys. Rev. Lett.* **122** (2019) 231802 [[arXiv:1903.03074](#)].
- [154] LHCb collaboration, *Model-independent measurement of charm mixing parameters in  $\bar{B} \rightarrow D^0 (\rightarrow K_S^0 \pi^+ \pi^-) \mu^- \bar{\nu}_\mu X$  decays*, [[arXiv:2208.06512](#)], submitted to *Phys. Rev. D*.
- [155] BELLE collaboration, *Measurement of  $y_{CP}$  in  $D^0$  meson decays to the  $K_S^0 K^+ K^-$  final state*, *Phys. Rev. D* **80** (2009) 052006 [[arXiv:0905.4185](#)].

- [156] BABAR collaboration, *Measurement of  $D^0 - \bar{D}^0$  mixing and CP violation in two-body  $D^0$  decays*, *Phys. Rev. D* **87** (2013) 012004 [[arXiv:1209.3896](#)].
- [157] BELLE collaboration, *Measurement of  $D^0 - \bar{D}^0$  mixing and search for CP violation in  $D^0 \rightarrow K^+K^-, \pi^+\pi^-$  decays with the full Belle data set*, *Phys. Lett. B* **753** (2016) 412 [[arXiv:1509.08266](#)].
- [158] LHCb collaboration, *Measurement of the charm-mixing parameter  $y_{CP}$* , *Phys. Rev. Lett.* **122** (2019) 011802 [[arXiv:1810.06874](#)].
- [159] BELLE collaboration, *Measurement of the charm-mixing parameter  $y_{CP}$  in  $D^0 \rightarrow K_S^0 \omega$  decays at Belle*, *Phys. Rev. D* **102** (2020) 071102 [[arXiv:1912.10912](#)].
- [160] G.M. Pietrzyk, *Precision measurement of neutral charm meson mixing parameters*, Ph.D. thesis, École Polytechnique Fédérale de Lausanne, 2021, [CERN-THESIS-2021-295](#).
- [161] M.W. Kenzie and V. Gligorov, *Lifetime unbiased beauty and charm triggers at LHCb*, [LHCb-PUB-2015-026](#), 2016.
- [162] M. Rama, *Effect of  $D-\bar{D}$  mixing in the extraction of  $\gamma$  with  $B^- \rightarrow D^0 K^-$  and  $B^- \rightarrow D^0 \pi^-$  decays*, *Phys. Rev. D* **89** (2014) 014021 [[arXiv:1307.4384](#)].
- [163] LHCb collaboration, *Measurement of CP observables in  $B^\pm \rightarrow D^{(*)} K^\pm$  and  $B^\pm \rightarrow D^{(*)} \pi^\pm$  decays using two-body D final states*, *JHEP* **04** (2021) 081 [[arXiv:2012.09903](#)].
- [164] LHCb collaboration, *Measurement of the CKM angle  $\gamma$  in  $B^\pm \rightarrow DK^\pm$  and  $B^\pm \rightarrow D\pi^\pm$  decays with  $D \rightarrow K_S h^+ h^-$* , *JHEP* **02** (2021) 0169 [[arXiv:2010.08483](#)].
- [165] D. Atwood, I. Dunietz and A. Soni, *Improved methods for observing CP violation in  $B^+ \rightarrow KD$  and measuring the CKM phase  $\gamma$* , *Phys. Rev. D* **63** (2001) 036005 [[hep-ph/0008090](#)].
- [166] A. Giri, Y. Grossman, A. Soffer and J. Zupan, *Determining  $\gamma$  using  $B^\pm \rightarrow DK^\pm$  with multibody D decays*, *Phys. Rev. D* **68** (2003) 054018 [[hep-ph/0303187](#)].
- [167] BESIII collaboration, *Measurement of the  $D \rightarrow K^- \pi^+ \pi^+ \pi^-$  and  $D \rightarrow K^- \pi^+ \pi^0$  coherence factors and average strong-phase differences in quantum-correlated  $D\bar{D}$  decays*, *JHEP* **05** (2021) 164 [[arXiv:2103.05988](#)].
- [168] S. Harnew and J. Rademacker, *Model independent determination of the CKM phase  $\gamma$  using input from  $D^0 - \bar{D}^0$  mixing*, *JHEP* **03** (2015) 169 [[arXiv:1412.7254](#)].
- [169] T. Evans, J. Libby, S. Malde and G. Wilkinson, *Improved sensitivity to the CKM phase  $\gamma$  through binning phase space in  $B^- \rightarrow DK^-, D \rightarrow K^+ \pi^- \pi^- \pi^+$  decays*, *Phys. Lett. B* **802** (2020) 135188 [[arXiv:1909.10196](#)].
- [170] BELLE II collaboration, *The Belle II physics book*, *PTEP* **2019** 123C01 [Erratum *ibid* **24** (2020) 029201] [[arXiv:1808.10567](#)], pp. 379–388.
- [171] BESIII collaboration, *Future Physics Programme of BESIII*, *Chin. Phys. C* **44** (2020) 040001 [[arXiv:1912.05983](#)].
- [172] S. Eidelman, *Project of the Super-tau-charm Factory in Novosibirsk*, *Nucl. Part. Phys. Proc.* **260** (2015) 238.
- [173] Q. Luo, W. Gao, J. Lan, W. Li and D. Xu, *Progress of conceptual study for the accelerators of a 2–7 GeV Super Tau Charm Facility at China*, in *10th International Particle Accelerator Conference*, p. MOPRB031, 2019, [DOI](#).
- [174] LHCb collaboration, *Expression of Interest for a Phase-II LHCb Upgrade: Opportunities in flavour physics, and beyond, in the HL-LHC era*, [CERN-LHCC-2017-003](#), 2017.
- [175] LHCb collaboration, *Physics case for an LHCb Upgrade II — Opportunities in flavour physics, and beyond, in the HL-LHC era*, [CERN-LHCC-2018-027](#), 2018, [[arXiv:1808.08865](#)].

- [176] J.J. Aubert et al., *Experimental observation of a heavy particle J*, *Phys. Rev. Lett.* **33** (1974) 1404.
- [177] J.E. Augustin et al., *Discovery of a narrow resonance in  $e^+e^-$  annihilation*, *Phys. Rev. Lett.* **33** (1974) 1406.
- [178] S. Bianco, F.L. Fabbri, D. Benson and I. Bigi, *A Cicerone for the physics of charm*, *Riv. Nuovo Cim.* **26** (2003) 1 [[hep-ex/0309021](#)].